

# From Bifurcations to State-Variable Statistics in Isotropic Turbulence: Internal Structure, Intermittency, and Kolmogorov Scaling via Non-Observable Quasi-PDFs

Nicola de Divitiis

*"La Sapienza" University, Dipartimento di Ingegneria Meccanica e Aerospaziale, Via  
Eudossiana, 18, 00184 Rome, Italy,  
phone: +39-0644585268, fax: +39-0644585750,  
e-mail: n.dedivitiis@gmail.com, nicola.dedivitiis@uniroma1.it*

---

## Abstract

This article investigates the intrinsic link between skewness and statistical intermittency in velocity and temperature increments within homogeneous isotropic turbulence. The theoretical framework builds upon the author's previously established closure schemes for the von Kármán–Howarth and Corrsin equations. A transition Taylor–scale Reynolds number is first estimated via a formal bifurcation analysis of the closed von Kármán–Howarth equation.

A central thesis of this work is that while the nonlinearity of the Navier–Stokes equations is fundamentally responsible for the emergence of intermittency in velocity and temperature increments, it is insufficient on its own to recover the Kolmogorov scaling law. We demonstrate that the non-observability of bifurcation modes constitutes the missing conceptual link: the concomitant effect of nonlinearity and non-observability not only determines the Kolmogorov scaling and drives an intermittency that grows

monotonically with the Taylor–scale Reynolds number, but also enables the analytical determination of the internal structure functions of velocity and temperature differences, along with their corresponding PDFs and statistics.

By invoking the principle of the minimum number of parameters for statistical description, as introduced by Fisher (1922), we show that the entire statistics of velocity and temperature increments can be analytically derived. This approach relies on a decomposition into bifurcation modes which, being non-observable quantities, are governed by quasi-probability distribution functions (quasi-PDFs). By admitting negative values, the latter provide the formal mathematical basis required to also represent local energy backscatter.

Notably, the analysis recovers the Kolmogorov law –specifically the scaling of the ratio between the velocity standard deviation and the Kolmogorov velocity as  $R_\lambda^{1/2}$ – as a direct consequence of the non–observability of these modes. Furthermore, our analysis reveals that the bifurcation modes exhibit amplitudes whose third statistical moment scales as  $R_\lambda^{-3}$ . The results show excellent agreement with benchmark numerical and experimental data existing in the literature, confirming that the proposed bifurcation–based decomposition rigorously captures the multi–scale, intermittent nature of fully developed turbulence.

*Keywords:*

Bifurcation Mode, Non–Observable Quasi–PDF, Kolmogorov Law,  
Intermittency

---

## 1. Introduction

The statistical description of fully developed turbulence remains one of the most formidable challenges in classical physics. Central to this endeavor is the concept of the energy cascade, a phenomenon originally envisioned by Richardson [1] and later formalized by Kolmogorov [2], wherein kinetic energy is transferred from large-scale injections to small-scale dissipative structures. Within this framework, the small-scale statistics are assumed to become isotropic and universal at sufficiently high Reynolds numbers. A rigorous mathematical cornerstone of this theory is the Kolmogorov 4/5 law, derived from the von Kármán–Howarth equation [3], which relates the third-order longitudinal structure function directly to the mean energy dissipation rate  $\epsilon$ .

As noted by Batchelor and Townsend [4], the non-zero value of the third-order moment implies a fundamental broken symmetry in the distribution of velocity increments, manifested as a persistent negative skewness. This skewness serves as the dynamical signature of the forward energy cascade and is intimately linked to the vortex stretching mechanism. However, decades of experimental and numerical research [5, 6, 7] have demonstrated that the self-similar scaling predicted by K41 is violated by internal intermittency. Recent extreme-resolution Direct Numerical Simulations (DNS) [8, 9] have further elucidated how the dissipation field is concentrated on small-scale, high-intensity structures, reinforcing the refined hypotheses of Kolmogorov [10] and Oboukhov [11].

The quest to quantify these departures led to the fractal and multifractal formalisms [12, 13] and subsequent dynamical models [14, 15]. Contemporary

investigations [16, 17] have highlighted the persistent difficulty in reconciling the local geometry of vortex tubes with the global statistical scaling. For passive scalars, such as temperature, the Corrsin–Oboukhov theory [18] often fails to capture the intense ramp-and-cliff structures and the extreme intermittency documented from classic studies [19, 20] to modern computational analyses [21].

Although skewness and intermittency have occupied a central role in the scientific literature, to the best of the author’s knowledge, an integrated analysis of these phenomena through the lens of bifurcation mode non-observability and Fisher’s principle of minimum free parameters [22] has not yet received the attention it deserves. The present work addresses this gap by situating the study of the link between skewness and intermittency within the framework of the closure schemes for the von Kármán–Howarth and Corrsin equations previously developed by the author in [23, 24, 25, 26].

Furthermore, a novel bifurcation analysis of the closed von Kármán–Howarth equation is proposed, which considers the route starting from fully developed turbulence toward non-chaotic regimes. This extends the discussion of previous works and represents an alternative point of view for studying the turbulent transition. According to this analysis, the closed von Kármán–Howarth equation is decomposed into several ordinary differential equations through the Taylor series expansion of the longitudinal velocity correlation. This procedure leads to an estimate of the Taylor-scale Reynolds number at the transition. This critical value is found to be approximately 10, which is in good agreement with several experimental observations. Notably, this result aligns closely with the bifurcation analysis of the energy cascade presented in

[23], which provides a critical Reynolds number of 10.13 assuming the route toward turbulence follows the Feigenbaum scenario [27, 28].

Subsequently, by leveraging the Navier–Stokes and heat equations, we analytically define and estimate velocity and temperature fluctuations as variations occurring over a time interval during which the quadratic form associated with the local fluid deformation remains definite in sign.

Building upon these definitions and the aforementioned closed correlation equations, this work rigorously derives the structure function scaling and the statistical distributions that were previously introduced on a heuristic basis in [23, 24, 29]. This analysis, supported by a formal bifurcation review of the energy cascade [30], suggests that while nonlinearity drives intermittency, it is the non-observability of bifurcation modes that constitutes the critical link for recovering Kolmogorov scaling. Importantly, the non-observability of these modes not only explains the Kolmogorov scaling and the intermittency increasing with the Taylor-scale Reynolds number, but above all, it allows for the determination of the internal structure functions for velocity and temperature differences, as well as the corresponding PDFs and statistics that closely match the existing experimental and numerical data in the literature.

By invoking Fisher’s principle of parsimony [22], we demonstrate that the complete statistics of velocity and temperature increments can be analytically derived through a decomposition into bifurcation modes. These modes are treated as non-observable quantities governed by quasi-PDFs. Notably, the proposed analysis reveals that the bifurcation modes exhibit a third-order statistical moment scaling as  $R_\lambda^{-3}$ . Consequently, the Kolmogorov scaling  $\sqrt{R_\lambda}$  is recovered as a direct manifestation of this non-observability, showing

excellent agreement with recent benchmark data [8, 31].

### Theoretical Basis: Correlation Equations and Nondiffusive Closures

The present analysis is strictly founded upon the closure schemes for the von Kármán–Howarth and Corrsin equations established by the author in [26]. In that work, the emergence of a Liouville spectral gap and the phenomenon of bifurcation-driven Lagrangian–Eulerian decoupling provided a physical-mathematical basis for nondiffusive turbulence closures. To ensure self-consistency, we recall the governing equations and the specific functional forms of the closures utilized herein.

In the context of homogeneous isotropic turbulence, the dynamical evolution of the longitudinal velocity correlation  $f = \langle u_r u_r' \rangle_E / u^2$  and the temperature correlation  $f_\theta = \langle \vartheta \vartheta' \rangle_E / \theta^2$  are governed by:

$$\begin{aligned} \frac{\partial f}{\partial t} &= \frac{K}{u^2} + 2\nu \left( \frac{\partial^2 f}{\partial r^2} + \frac{4}{r} \frac{\partial f}{\partial r} \right) + \frac{10\nu}{\lambda_T^2} f, \\ \frac{\partial f_\theta}{\partial t} &= \frac{K}{\theta^2} + 2\kappa \left( \frac{\partial^2 f_\theta}{\partial r^2} + \frac{2}{r} \frac{\partial f_\theta}{\partial r} \right) + \frac{12\kappa}{\lambda_\theta^2} f_\theta, \end{aligned} \tag{1}$$

where  $u \equiv \sqrt{\langle u_r^2 \rangle_E}$ ,  $\theta \equiv \sqrt{\langle \vartheta^2 \rangle_E}$ ,  $\langle \cdot \rangle_E$  denotes the average calculated over the Eulerian ensemble, and the quantities  $\lambda_T \equiv \sqrt{-1/f''(0)}$  and  $\lambda_\theta \equiv \sqrt{-2/f_\theta''(0)}$  are Taylor and Corrsin microscales, respectively. The functions  $K$  and  $G$ , which account for the turbulent energy cascade, are related to  $k$  and  $m^*$ , namely the longitudinal triple velocity correlation and the mixed

triple correlation between  $u_r$  and  $\vartheta$ , according to

$$K(r) = u^3 \left( \frac{\partial}{\partial r} + \frac{4}{r} \right) k(r), \quad \text{where } k(r) = \frac{\langle u_r^2 u_r' \rangle_E}{u^3}, \quad (2)$$

$$G(r) = 2u\theta^2 \left( \frac{\partial}{\partial r} + \frac{2}{r} \right) m^*(r), \quad \text{where } m^*(r) = \frac{\langle u_r \vartheta \vartheta' \rangle_E}{\theta^2 u},$$

Equations (1) are closed once both  $K$  and  $G$  are expressed solely in terms of  $f$  and  $f_\theta$ . Following the Liouville analysis of Ref. [26], the closures for  $K$  and  $G$  are given by:

$$K(r) = u^3 \sqrt{\frac{1-f}{2}} \frac{\partial f}{\partial r}, \quad (3)$$

$$G(r) = u\theta^2 \sqrt{\frac{1-f}{2}} \frac{\partial f_\theta}{\partial r},$$

These functional forms effectively replace the traditional eddy-diffusivity assumptions with a description based on the nonlinear interaction of bifurcation modes. As demonstrated in [26], these closures are non-diffusive in nature, as they arise from the decoupling of Lagrangian trajectories in the presence of a spectral gap.

For the results obtained using Eqs. (3), the reader is referred to the data reported in Refs. [23, 24, 32]. In particular, such Refs. demonstrate that Eqs. (3) provide an accurate description of the energy cascade, reproducing negative values of the skewness of velocity and temperature increments

$$H_{u3}(r) \equiv \frac{\langle (\Delta u_r)^3 \rangle}{\langle (\Delta u_r)^2 \rangle^{3/2}} = \frac{6k(r)}{(2(1-f(r)))^{3/2}} \quad (4)$$

$$H_{\theta3}(r) \equiv \frac{\langle (\Delta \vartheta)^2 \Delta u_r \rangle}{\langle (\Delta \vartheta)^2 \rangle \langle (\Delta u_r)^2 \rangle^{1/2}} = \frac{4m^*}{2(1-f_\theta(r))(2(1-f(r)))^{1/2}}$$

and, in particular,

$$H_{u3}(0) = \lim_{r \rightarrow 0} H_{u3}(r) = -\frac{3}{7},$$

$$H_{\theta3}(0) = \lim_{r \rightarrow 0} H_{\theta3}(r) = -\frac{1}{5},$$
(5)

in agreement with the literature [33, 34, 35, 36, 37, 38], with the Kolmogorov law, and with temperature spectra consistent with the theoretical arguments of Kolmogorov, Obukhov–Corrsin, and Batchelor [39, 40, 41], as well as with experimental [42, 43] and numerical [44, 45] results.

This work takes these closed equations (1), (3) and Eq. (5) as a point of departure to investigate the interplay between skewness and intermittency. By applying Fisher’s principle of parsimony [22] to the statistics generated by these closures, we demonstrate that the non-observability of the underlying bifurcation modes is the fundamental mechanism responsible for the recovery of the Kolmogorov scaling and the emergence of non-Gaussian statistics.

Although the second of Eqs. (3) is formulated for temperature correlation equation, the present analysis applies, without loss of generality, to any passive scalar with diffusive transport.

### **Mathematical Framework: Quasi-PDFs, Non-observable Bifurcation Modes and Fisher Parsimony Principle**

The analytical derivation of the statistics for velocity and temperature increments—the primary physical observables of the system—rests upon a decomposition into discrete bifurcation modes. Within this framework, while the state variables, velocity  $\mathbf{u}$  and temperature  $\vartheta$ , are directly accessible to

measurement, the individual bifurcation modes governing their multi-scale evolution remain inherently latent.

A fundamental distinction arises from their governing dynamics: while the observable field  $\mathbf{u}$  satisfies the Navier–Stokes equations, the individual bifurcation modes do not. These modes represent mathematical segregations of the fluid state that possess physical reality only in their collective combination. Consequently, such modes are fundamentally *non-observable*. According to Liouville’s theorem, the observable field  $\mathbf{u}$  obeys a classical, positive-definite distribution; conversely, the non-observable modes, emerging from this formal decomposition, are governed by quasi-probability density functions (quasi-PDFs) which may exhibit negative values [46, 47, 48]. The global statistical behavior emerges from the collective contribution of these latent modes, governed by the closure of the von Kármán–Howarth and Corrsin equations [23, 24, 26].

The mathematical necessity for quasi-PDFs to admit negative excursions stems from the physics of non-observability. This has profound implications for the energy cascade: specifically, the coexistence of negative and positive regions within the quasi-PDF provides the formal basis for representing local *backscatter*—the upscale transfer of kinetic energy. This phenomenon is a hallmark of the non-linear dynamics of the Navier–Stokes equations in fully developed turbulence. Accordingly, the total observed skewness of the velocity increments,  $H_{u3}(r)$ , can be analytically mapped onto the underlying quasi-PDF structure.

### *Non-observability and the Fisher Parsimony Principle*

The present theory posits that bifurcation modes are *non-observable* entities whose existence is inferred solely through the macroscopic statistics of resolved increments. Adhering to the principle of parsimony [22], which mandates a sufficient statistical description via a minimal set of parameters, we demonstrate that turbulent complexity is minimized through the selection of a specific, irreducible set of modes.

This non-observability constitutes the critical conceptual link between intrinsic non-linearity and the recovery of Kolmogorov scaling. By requiring the statistical description to be compatible with a minimal set of free parameters in the Fisherian sense, the model constrains the PDFs of  $\Delta u_r$  and  $\Delta\vartheta$ . This constraint, in conjunction with the Navier–Stokes non-linearity, leads directly to the analytical prediction of intermittency, which increases monotonically with  $R_\lambda$ . Furthermore, it recovers the Kolmogorov law, whereby the standard deviation of observable increments scales as  $\langle(\Delta u_r)^2\rangle^{1/2}/u_K \propto \sqrt{R_\lambda}$  ( $u_K$  being the Kolmogorov velocity).

Crucially, while the Navier–Stokes non-linearity inherently implies the existence of intermittency, it is the non-observability of the bifurcation modes that enforces the Kolmogorov scaling. In this perspective, intermittency that increases with  $R_\lambda$  is not an *ad hoc* correction, but rather the unique statistically consistent state emerging from the non-observability of bifurcation modes and the constant skewness of  $\Delta u_r$ , under the rigorous constraint of parsimony. Moreover, this mechanism also induces an intermittency of the temperature difference which rises accordingly with the Péclet number.

## 2. Bifurcation analysis and Transition Reynolds number: from fully developed turbulence toward non-chaotic regimes.

The transition toward fully developed turbulence traditionally proceeds from non-chaotic regimes via intermediate stages [49, 27, 50, 28], corresponding to successive bifurcations at comparable Reynolds scales. In a departure from this classical route to chaos, this section investigates the inverse route: we examine the loss of stability as the system evolves from fully developed homogeneous isotropic turbulence toward a non-chaotic state. Along this path, characterized by a progressive reduction in the Taylor-scale Reynolds number, we analyze the bifurcations inherent in the closed von Kármán–Howarth equation. This framework allows for the estimation of a critical threshold,  $R_T^*$ , which represents the minimum  $R_\lambda$  necessary to sustain a fully developed, homogeneous, and isotropic turbulent state. The bifurcation analysis of the velocity correlation is formulated by expanding  $f(t, r) = \sum_k f_0^{(k)} r^k / k!$  into an even Taylor series. The evolution of the resulting coefficients is governed by a system of coupled equations, where each coefficient corresponds to a

specific dynamical degree of freedom

$$\left\{ \begin{array}{l} \frac{du}{dt} = -5\nu \frac{u}{\lambda_T^2}, \\ \frac{d\lambda_T}{dt} = -\frac{u}{2} + \frac{\nu}{\lambda_T} \left( \frac{7}{3} f_0^{IV} \lambda_T^4 - 5 \right), \\ \frac{df_0^{IV}}{dt} = \dots, \\ \dots \\ \frac{df_0^{(n)}}{dt} = \dots, \\ \dots \end{array} \right. \quad (6)$$

Such equations can be written by introducing the infinite dimensional state vector

$$\mathbf{f} \equiv \left( u, \lambda_T, f_0^{IV}, \dots, f_0^{(n)}, \dots \right). \quad (7)$$

which represents the state of the longitudinal velocity correlation. Therefore, Eqs. (6), formally written as

$$\dot{\mathbf{f}} = \mathbf{F}(\mathbf{f}, \nu) \quad (8)$$

are equivalent to the closed von Kármán–Howarth equation. Equation (8) defines a bifurcation problem where  $\nu$  plays the role of control parameter. Thus, this bifurcation analysis studies the variations of  $\mathbf{f}$  caused by  $\nu$  according to

$$\mathbf{F}(\mathbf{f}, \nu) = \mathbf{F}(\mathbf{f}_0, \nu_0) \quad (9)$$

starting from  $\mathbf{f}_0, \nu_0$ . For  $\nu > \nu_0$ ,  $\mathbf{f}$  is formally calculated through the implicit functions inversion theorem

$$\mathbf{f} = \mathbf{G}(\mathbf{f}_0, \nu_0, \nu) \equiv \mathbf{f}_0 - \int_{\nu_0}^{\nu} (\nabla_{\mathbf{f}}\mathbf{F})^{-1} \frac{\partial \mathbf{F}}{\partial \nu} d\nu \quad (10)$$

where  $\nabla_{\mathbf{f}}\mathbf{F}$  is the jacobian  $\partial \mathbf{F} / \partial \mathbf{f}$ . A bifurcation of Eq. (8) happens when this jacobian is singular, i.e.

$$\det(\nabla_{\mathbf{f}}\mathbf{F}) = 0 \quad (11)$$

In the limit of vanishingly small  $\nu_0$  (corresponding to sufficiently large  $R_T$ ), the energy cascade dominates viscous effects, ensuring the non-singularity of the Jacobian  $\nabla_{\mathbf{f}}\mathbf{F}$ . As  $\nu$  increases, the state vector  $\mathbf{f}$  evolves smoothly according to Eq. (10) until dissipation progressively overwhelms the energy cascade, leading to the primary bifurcation defined by condition (11). At this critical juncture, a 'hard' loss of stability occurs, marking the collapse of fully developed turbulence toward non-chaotic regimes [51]. Consequently, the threshold  $R_T^*$  is identified as the value at bifurcation that maximizes the largest real part of the eigenvalues of  $\nabla_{\mathbf{f}}\mathbf{F}$  [52, 51], consistent with the prescribed average kinetic energy  $u^2$ , namely

$$R_{\lambda}^* \mid \sup_k \{\Re(l_k)\} = \max, \quad (12)$$

$$\det(\nabla_{\mathbf{f}}\mathbf{F}) = 0,$$

$$u^2 = \text{given}$$

this is a constrained extremum condition, where  $l_k, k=1, 2, \dots$  are the eigenvalues of  $\nabla_{\mathbf{f}}\mathbf{F}$ . We assume that the phase space of Eq. (8), while inherently

infinite-dimensional, can be effectively projected onto a finite-dimensional manifold. Within this framework, Eqs. (8) are mapped into the dynamical systems paradigm pioneered by Ruelle and Takens [49], allowing the governing equations to be analyzed through the lens of classical bifurcation theory for ordinary differential equations. Mathematically, this transition is justified by the convergence of the functional series representing the solution; provided that the truncation satisfies uniform convergence criteria (e.g., the Weierstrass M-test), the bifurcation analysis remains asymptotically consistent with the full operator dynamics. The omitted degrees of freedom, residing in the series "tail," do not qualitatively alter the stability or the branching evolution of the solutions.

From the perspective of the laminar–turbulent transition, this reduction is further substantiated by the existence of a local center manifold. The onset of instability is driven by a discrete set of critical modes that dictate the qualitative changes in flow topology, while the remaining infinite degrees of freedom exhibit sufficiently strong decay to be treated as enslaved to the primary dynamics. This effectively compresses the infinite-dimensional phase space into its most influential components without compromising the underlying bifurcation structure.

Physically, the energy cascade primarily drives the temporal reduction of  $\lambda_T$  while  $f$  maintains a self-similar profile. This suggests that, in the proximity of the transition, the variables  $u$  and  $\lambda_T$  provide a sufficient descriptor for the evolution of  $f$ . Consequently, the state vector  $\mathbf{f}$  is truncated to its first two components, corresponding to the  $r^0$  and  $r^2$  terms in Eqs. (6). Leveraging this self-similarity, the infinite–dimensional space is replaced by

a low-dimensional manifold, where the state vector reduces to:

$$\mathbf{f} \equiv (u, \lambda_T), \quad (13)$$

Thus, the jacobian  $\nabla_{\mathbf{f}}\mathbf{F}$  is reduced to

$$\nabla_{\mathbf{f}}\mathbf{F} = \begin{pmatrix} \frac{\partial \dot{u}}{\partial u} & \frac{\partial \dot{u}}{\partial \lambda_T} \\ \frac{\partial \dot{\lambda}_T}{\partial u} & \frac{\partial \dot{\lambda}_T}{\partial \lambda_T} \end{pmatrix} \quad (14)$$

whose determinant is

$$\det(\nabla_{\mathbf{f}}\mathbf{F}) = -\frac{5\nu^2}{\lambda_T^2} \left( 7f_0^{IV}\lambda_T^2 + \frac{10}{\lambda_T^2} \right) + 5\nu\frac{u}{\lambda_T^3} \quad (15)$$

where  $f_0^{IV}$  plays the role of a variable in the constrained extremum condition (12). Equation (15) implies that  $\det(\nabla_{\mathbf{f}}\mathbf{F}) > 0$  for sufficiently small  $\nu > 0$ . The emergence of a bifurcation requires the vanishing of the Jacobian determinant, which imposes the condition  $f_0^{IV}\lambda_T^4 > -10/7$ . As  $\nu$  increases, the ratio  $\det(\nabla_{\mathbf{f}}\mathbf{F})/\nu$  monotonically decreases until it reaches a singular point. To determine the critical threshold  $R_\lambda^*$ , we eliminate  $f_0^{IV}$  by invoking the bifurcation condition  $\det(\nabla_{\mathbf{f}}\mathbf{F}) = 0$  in Eq. (15), yielding:

$$f_0^{IV} = \frac{1}{7\lambda_T^2\nu} \left( \frac{u}{\lambda_T} - 10\frac{\nu}{\lambda_T^2} \right) \quad (16)$$

The resulting singular Jacobian is given by:

$$\nabla_{\mathbf{f}}\mathbf{F} = \begin{pmatrix} -5\nu/\lambda_T^2 & 10\nu u/\lambda_T^3 \\ -1/2 & u/\lambda_T \end{pmatrix} \quad (17)$$

which admits the eigenvalues  $l_1, l_2$  and corresponding eigenvectors  $\mathbf{y}_1, \mathbf{y}_2$ :

$$l_1 = 0, \quad \mathbf{y}_1 = \left( u, \frac{\lambda_T}{2} \right) \tag{18}$$

$$l_2 = \frac{u^2}{\nu} \left( \frac{1}{R_\lambda} - \frac{5}{R_\lambda^2} \right), \quad \mathbf{y}_2 = \left( u, R_\lambda \frac{\lambda_T}{10} \right)$$

The real eigenvalue  $l_2$  remains positive for  $R_\lambda > 5$  and attains its maximum,  $l_{2,max} = 5\nu/\lambda_T^2$ , at  $R_\lambda = 10$ . Consequently, we estimate the critical Taylor-scale Reynolds number as:

$$R_\lambda^* = 10 \tag{19}$$

corresponding to  $f_0^{IV} = 0$ .

A further characteristic threshold is identified when both eigenvalues vanish at  $R_\lambda = 5$ , marking the onset of the decaying turbulence regime. In this limit, the evolution of  $f$  and  $\lambda_T$  is well-approximated by:

$$\frac{d\lambda_T}{dt} \simeq 0, \quad f \simeq \exp \left( -\frac{1}{2} \left( \frac{r}{\lambda_T} \right)^2 \right) \tag{20}$$

leading to  $f_0^{IV} \lambda_T^4 \simeq 3$  and  $R_\lambda \simeq 4$ , which is consistent with the aforementioned estimation.

The value  $R_\lambda^*$  represents the lower bound for sustaining fully developed, homogeneous, and isotropic turbulence, thereby establishing the order of magnitude for the transition. While the actual route to chaos involves intermediate Navier–Stokes bifurcations where isotropy and homogeneity may not yet be established, this analysis suggests that during transition,  $R_\lambda$  spans the range:

$$4 \lesssim R_\lambda \lesssim 10 \tag{21}$$

The estimated value  $R_\lambda^* = 10$  is in excellent agreement with bifurcation analyses of the turbulent energy cascade [53], which show that if the cascade follows the Feigenbaum scenario [27, 28], a critical Taylor–scale Reynolds number of approximately 10.13 emerges after three successive bifurcations.

In summary, the estimation of  $R_\lambda^*$  is predicated on the local self–similarity induced by the closures (3), which justifies the reduction of the infinite-dimensional system to the primary two-equation manifold in (6).

### 3. Velocity and temperature fluctuations

This section aims to derive formal expressions for Eulerian velocity and temperature fluctuations in fully developed turbulence, providing a rigorous basis for estimating the statistical properties of these fields. The derivation leverages the Lyapunov theory of Lagrangian trajectories, as established in [26], by employing a dual framework of referential and spatial coordinates.

For analytical convenience, the Navier–Stokes and heat equations are cast into the following divergence form:

$$\left\{ \begin{array}{l} \frac{\partial \mathbf{u}}{\partial t} = \frac{1}{\rho} \nabla_{\mathbf{x}} \cdot \hat{\mathbf{T}} \\ \frac{\partial \vartheta}{\partial t} = -\frac{1}{c\rho} \nabla_{\mathbf{x}} \cdot \hat{\mathbf{q}} \end{array} \right. \quad (22)$$

where the total flux tensors,  $\hat{\mathbf{T}}$  and  $\hat{\mathbf{q}}$ , are defined as:

$$\hat{\mathbf{T}} = \mathbf{T} - \rho \mathbf{u} \otimes \mathbf{u}, \quad \hat{\mathbf{q}} = \mathbf{q} + c\rho \mathbf{u} \vartheta \quad (23)$$

In this context,  $\mathbf{T}$  and  $\mathbf{q}$  denote the stress tensor and heat flux, respectively,

which satisfy the Navier–Fourier constitutive relations:

$$\mathbf{T} = -\mathbf{I}p + \mathbf{T}_v, \quad \mathbf{q} = -\kappa\nabla_{\mathbf{x}}\vartheta, \quad \mathbf{T}_v = \mu(\nabla_{\mathbf{x}}\mathbf{u} + \nabla_{\mathbf{x}}\mathbf{u}^T) \quad (24)$$

where the spatial gradients are evaluated with respect to the Eulerian coordinates  $\mathbf{x}$  [54]. Here,  $\mathbf{I}$  is the identity tensor,  $\mathbf{T}_v$  is the viscous stress tensor, while  $\mu, \kappa, c$ , and  $\rho$  represent the dynamic viscosity, thermal conductivity, specific heat, and density, respectively—all treated as constant quantities. The pressure  $p$  is determined via the continuity equation and expressed as a functional of the velocity field:

$$p(t, \mathbf{x}) = \frac{\rho}{4\pi} \int \frac{\partial^2 u'_i u'_j}{\partial x'_i \partial x'_j} \frac{dV(\mathbf{x}')}{|\mathbf{x}' - \mathbf{x}|} \quad (25)$$

This formulation explicitly accounts for non-local effects [55], effectively reducing the Navier–Stokes equations to an integro–differential system.

Velocity and temperature fluctuations are defined as variations occurring over a time interval  $(t_0, t)$  such that the quadratic form associated with the local deformation gradient  $\partial\mathbf{x}/\partial\mathbf{X}$  maintains a constant sign, where  $\mathbf{X}$  denotes the referential (Lagrangian) coordinate. By applying the Lyapunov theory of Lagrangian trajectories, Eqs. (22) are transformed using the referential coordinates and the local fluid deformation:

$$\frac{\partial\mathbf{u}}{\partial t} = \frac{1}{\rho} \frac{\partial\hat{\mathbf{T}}}{\partial\mathbf{X}} \left( \frac{\partial\mathbf{x}}{\partial\mathbf{X}} \right)^{-1}, \quad \frac{\partial\vartheta}{\partial t} = -\frac{1}{c\rho} \frac{\partial\hat{\mathbf{q}}}{\partial\mathbf{X}} \left( \frac{\partial\mathbf{x}}{\partial\mathbf{X}} \right)^{-1} \quad (26)$$

The inverse deformation gradient

$$\mathbf{G} = \left( \frac{\partial\mathbf{x}}{\partial\mathbf{X}} \right)^{-1} \quad (27)$$

is defined such that  $\mathbf{G}(t_0) = \mathbf{I}$ .

The simultaneous adoption of referential and spatial coordinates enables the factorization of  $\partial\mathbf{u}/\partial t$  and  $\partial\vartheta/\partial t$  into a product of two matrices characterized by disparate time scales: one governed by the Eulerian velocity and temperature fields, and the other representing the local fluid distortion. Following [26],  $\mathbf{G}$  evolves according to Lyapunov theory, while the Lagrangian gradients  $\partial\hat{\mathbf{T}}/\partial\mathbf{X}$  and  $\partial\hat{\mathbf{q}}/\partial\mathbf{X}$  exhibit a slow-growth property. Consequently, fluctuations are defined over a time interval during which the quadratic form associated with  $\mathbf{G}$  remains definite in sign. Hence, the velocity and temperature fluctuations are expressed as:

$$\mathbf{u} = \frac{1}{\rho} \int_{t_0}^t \left( \frac{\partial\hat{\mathbf{T}}}{\partial\mathbf{X}} \right)_{\tau} \left( \frac{\partial\mathbf{x}}{\partial\mathbf{X}} \right)_{\tau}^{-1} d\tau, \quad \vartheta = -\frac{1}{c\rho} \int_{t_0}^t \left( \frac{\partial\hat{\mathbf{q}}}{\partial\mathbf{X}} \right)_{\tau} \left( \frac{\partial\mathbf{x}}{\partial\mathbf{X}} \right)_{\tau}^{-1} d\tau \quad (28)$$

where the subscript  $\tau$  indicates the time at which the quantities are evaluated, and  $\mathbf{X}$  denotes the Lagrangian coordinate calculated at time  $t_0$  according to  $\mathbf{X} = \boldsymbol{\chi}^{-1}(\tau, \mathbf{x})$  with  $\tau \in (t_0, t)$  [54]. As the quadratic form associated with  $\partial\mathbf{x}/\partial\mathbf{X}$  preserves its sign within the interval  $(t_0, t)$ , the integral mean value theorem can be applied to Eqs. (28), yielding:

$$\exists t_U, t_{\Theta} \in (t_0, t) \mid \mathbf{u} = \frac{1}{\rho} \left( \frac{\partial\hat{\mathbf{T}}}{\partial\mathbf{X}} \right)_{t_U} \mathbf{W}, \quad \vartheta = -\frac{1}{c\rho} \left( \frac{\partial\hat{\mathbf{q}}}{\partial\mathbf{X}} \right)_{t_{\Theta}} \mathbf{W}, \quad (29)$$

where the matrix  $\mathbf{W}$  is defined as:

$$\mathbf{W} = \int_{t_0}^t \mathbf{G} d\tau \quad (30)$$

In conclusion, for developed turbulence, Eqs. (29) represent exact relations derived by integrating spatial and referential coordinates with local deformation. This provides a robust analytical framework for describing fluctuation dynamics and constitutes a fundamental starting point for characterizing the statistics of velocity and temperature fields in developed turbulence.

#### 4. Velocity and temperature difference and non-observable bifurcation modes

In developed turbulence, the longitudinal velocity and temperature increments,  $\Delta u_r = (\mathbf{u}(t, \mathbf{x}') - \mathbf{u}(t, \mathbf{x})) \cdot \mathbf{r}/r$  and  $\Delta \vartheta = \vartheta(t, \mathbf{x}') - \vartheta(t, \mathbf{x})$  with  $\mathbf{r} = \mathbf{x}' - \mathbf{x}$ , are of paramount importance, as they encapsulate the dynamics of the energy cascade, intermittency, and turbulent dissipation. This section employs the Navier–Stokes and heat equations, as summarized by (29), to analyze the analytical structure of  $\Delta u_r$  and  $\Delta \vartheta$  in fully developed homogeneous isotropic turbulence. This is achieved by leveraging the previously established Lagrangian Lyapunov framework alongside a specific statistical decomposition that accounts for bifurcation-induced effects. Specifically, within the present framework,  $\Delta u_r$  and  $\Delta \vartheta$  are decomposed into bifurcation modes. These modes represent non-observable quantities, each statistically characterized by a quasi-PDF. Such distributions may exhibit impulsive profiles and admit negative values, reflecting their nature as signed measures rather than classical probability densities. We demonstrate that a specific choice of these quasi-PDFs identically satisfies Eqs. (4)–(5), which define the dimensionless third-order statistical moments of  $\Delta u_r$  and  $\Delta \vartheta$ .

To analyze this, we first examine the impact of Navier–Stokes bifurcations on  $\Delta u_r$  and  $\Delta \vartheta$ . Using the fluctuation relations derived in Eq. (29), the increments are expressed in terms of the instantaneous velocity and tem-

perature fields as:

$$\begin{aligned}\Delta u_r &= \frac{1}{\rho} \left( \frac{\partial \hat{T}_{ij}}{\partial x_{0k}} \right)'_{t'_U} W'_{jk} - \frac{1}{\rho} \left( \frac{\partial \hat{T}_{ij}}{\partial x_{0k}} \right)_{t_U} W_{jk} \\ \Delta \vartheta &= -\frac{1}{c\rho} \left( \frac{\partial \hat{q}_j}{\partial x_{0k}} \right)'_{t'_\Theta} W'_{jk} + \frac{1}{c\rho} \left( \frac{\partial \hat{q}_j}{\partial x_{0k}} \right)_{t_\Theta} W_{jk}\end{aligned}\tag{31}$$

The sequence of bifurcations encountered during the fluid motion results in a continuous doubling of the velocity field into multiple components, denoted as  $\hat{\mathbf{v}}_k$  for  $k = 1, 2, \dots$ . Each bifurcation introduces new functions whose characteristics are statistically independent of the velocity field at preceding times. Consequently, the velocity field is decomposed as:

$$\mathbf{u}(t, \mathbf{x}) = \sum_k \hat{\mathbf{v}}_k(t, \mathbf{x})\tag{32}$$

It is crucial to remark that while the total field  $\mathbf{u}(t, \mathbf{x})$  satisfies the Navier–Stokes equations, the individual components  $\hat{\mathbf{v}}_k$  do not. These functions represent bifurcation modes, mathematical segregations of the fluid state that physically exist only in combination. As such, these modes are fundamentally non-observable. According to Liouville’s theorem, the observable field  $\mathbf{u}$  follows a classical, positive-definite distribution. Conversely, the non-observable modes  $\hat{\mathbf{v}}_k$ , resulting from this mathematical segregation, are governed by quasi-PDFs which may exhibit negative values [46, 47, 48].

The form of these quasi-PDFs is dictated by the Navier–Stokes bifurcations and the isotropy hypothesis. Regarding the former, for pressure and inertia to drive significant variations in velocity autocorrelation, each mode  $\hat{\mathbf{v}}_k = (\hat{v}_1, \hat{v}_2, \hat{v}_3)$  must follow a highly non-symmetric distribution, character-

ized by:

$$\frac{|\langle \hat{v}_{ki}^3 \rangle|}{\langle \hat{v}_{ki}^2 \rangle^{3/2}} \gg 1, \quad i = 1, 2, 3 \quad (33)$$

Simultaneously, under the isotropy hypothesis,  $\mathbf{u}$  would typically follow a Gaussian distribution [56], wherein inertia and pressure do not contribute to the time derivative of the third statistical moment. To reconcile this with the energy cascade, the third moments of  $\hat{\mathbf{v}}_k$  are expected to dominate the higher-order statistics:

$$\frac{|\langle \hat{v}_{ki}^3 \rangle|}{\langle \hat{v}_{ki}^2 \rangle^{3/2}} \gg \frac{|\langle \hat{v}_{ki}^4 \rangle|}{\langle \hat{v}_{ki}^2 \rangle^2}, \quad i = 1, 2, 3 \quad (34)$$

This framework justifies the representation of the velocity field  $\mathbf{u}$  and the passive scalar  $\vartheta$  as linear combinations of stochastic variables  $\xi_k$ , which effectively encapsulate the doubling effect characteristic of bifurcations:

$$\mathbf{u} = \sum_k \mathbf{U}_k \xi_k, \quad (35)$$

$$\vartheta = \sum_k \Theta_k \xi_k$$

where the spatial modes  $\mathbf{U}_k$  and  $\Theta_k$  satisfy the incompressibility constraint  $\nabla_{\mathbf{x}} \cdot \mathbf{U}_k = 0$ , and  $\xi_k$  denote independent centered stochastic variables. The quasi-PDF  $\hat{\delta}(\xi_k)$ , consistent with Eqs. (33) and (34), is formulated via a singular Gram–Charlier expansion truncated at the third order, developed around a nascent delta function  $\delta_e(\xi_k)$ :

$$\hat{\delta}(\xi_k) = \delta_e(\xi_k) - \frac{\langle \xi_k^3 \rangle}{3!} \delta^{(3)}(\xi_k) \quad (36)$$

In this construction, the standard deviation of  $\delta_e(\xi_k)$  is assumed to be infinitesimal yet non-vanishing, thereby ensuring the formal applicability of

the Central Limit Theorem (CLT) under summation. This specific expansion characterizes a physical regime in which the mode exhibits a dominant energy flux ( $|\langle \xi_k^3 \rangle| \gg 1$  and  $|\langle \xi_k^3 \rangle| \gg \langle \xi_k^2 \rangle$ ) while maintaining a vanishing local energy contribution, as evidenced by the infinitesimal variance. The inclusion of the third-order derivative of the Dirac delta implies that the mode serves exclusively as a vehicle for the turbulent cascade, redistributing energy across the spectrum without contributing to the local energy density—a defining feature of non-observable bifurcation modes in fully developed turbulence.

$$\langle \xi_k \rangle = 0, \quad \langle \xi_i \xi_j \xi_k \rangle = \begin{cases} q \neq 0, \forall i = j = k \\ 0 \text{ else} \end{cases} \quad (37)$$

where  $q$ , providing the skewness of  $\xi_k$   $k=1, 2, \dots$ , satisfies to

$$|q| \gg \langle \xi_k^n \rangle, \forall n \neq 3, \quad k = 1, 2, \dots, \quad (38)$$

**Remark.** *While the formal representation (35) might superficially resemble a Karhunen Loève Expansion (KLE) [57], it departs from it in two fundamental aspects that are crucial for the description of the Navier-Stokes bifurcation cascade. First, unlike the observable modes in a standard KLE, the variables  $\xi_k$  here represent non-observable bifurcation states. According to the Center Manifold Theory [58], near a bifurcation point, the system's dynamics are slaved to critical modes. In our framework, these modes are segregated: they represent pure energy transfer states rather than directly measurable velocity fluctuations. Second, the stochastic nature of each mode is described by a quasi-PDF rather than a classical probability density. Following the intuition*

of Feynman [46] on negative probabilities for intermediate states, each  $\xi_k$  is governed by a singular Gram-Charlier expansion (36). This formulation allows for the mathematical representation of intermittency and local energy flux without violating the global Gaussianity of the system, which is recovered in the limit of large  $N$  through the Lindeberg-Feller condition [59].

Through the decomposition in Eq. (35), we demonstrate that the negative value of  $H_u^{(3)}(r)$  carries profound implications for the statistical properties of  $\Delta u_r$  and  $\Delta \vartheta$ , particularly concerning the emergence of intermittency as the Taylor-scale Reynolds and Péclet numbers increase. To investigate this, we first derive the analytical fluctuations of  $u_i$  and  $\vartheta$  in terms of the bifurcation variables  $\xi_k$  by substituting Eq. (35) into Eq. (29). Hence, dimensionless eulerian velocity and temperature fluctuations read as

$$\begin{cases} u_i = \sum_j \sum_k A_{jk}^{(i)} \xi_j \xi_k + \frac{1}{R_\lambda} \sum_k a_k^{(i)} \xi_k, & i = 1, 2, 3 \\ \vartheta = \sum_j \sum_k B_{jk} \xi_j \xi_k + \frac{1}{Pe} \sum_k b_k \xi_k \end{cases} \quad (39)$$

where the equations were non-dimensionalized using the standard deviations of velocity and temperature, along with the corresponding Taylor and Corrsin correlation scales, thus  $R_\lambda = u\lambda_T/\nu$ ,  $Pe = R_\lambda Pr$ ,  $Pr = \nu/\alpha$ ,  $\alpha = \kappa/(c\rho)$ . In this formulation, the quadratic forms  $\sum \sum A_{jk}^{(i)} \xi_j \xi_k$  and the linear terms  $1/R_\lambda \sum a_k^{(i)} \xi_k$  represent the contributions of inertial/pressure forces and fluid viscosity, respectively. Similarly, for the passive scalar  $\vartheta$ , the terms arise from convective transport and thermal conduction.

Under the hypothesis of turbulent isotropy, the velocity  $u_i$  and temperature  $\vartheta$  are expected to behave as Gaussian stochastic variables [56, 59, 60].

Physically, this implies that the vast number of independent bifurcation modes  $\xi_k$  contributing to the global field satisfy the Lindeberg condition, a necessary and sufficient requirement for the Central Limit Theorem (CLT) to hold [59, 60]. Crucially, this condition remains valid even for singular quasi-PDFs, as the infinitesimal contribution of each individual non-observable mode ensures a convergent Gaussian macroscopic state. Specifically, the second terms on the right-hand side (RHS) of Eqs. (39) are sums of uncorrelated variables described by quasi-PDFs, where both  $a_k^{(i)}$  and  $b_k$  satisfy the Lindeberg condition. The first terms are quadratic forms where, due to isotropy, the structure of the matrices  $A_{jk}^{(i)}$  and  $B_{jk}$  is such that their spectral radii are negligible with respect to the corresponding Frobenius norms. This constitutes a necessary and sufficient condition for  $u$  and  $\vartheta$  to be distributed according to Gaussian PDFs [61].

However, the CLT does not extend to the increments  $\Delta u_i$  and  $\Delta \vartheta$ . Since these quantities result from the difference between two highly correlated Gaussian fields, the subtraction process effectively filters out the uncorrelated Gaussian background, thereby exposing the underlying singular structure of the bifurcation modes. In this scale-selective regime, the Lindeberg condition is no longer satisfied, and the PDF of the increments deviates significantly from a Gaussian distribution, manifesting the observed intermittency. To characterize this statistical behavior, the fluctuations of the increments are

expressed as:

$$\begin{aligned}\Delta u_r(\mathbf{r}) &= \sum_j \sum_k \Delta A_{jk} \xi_j \xi_k + \frac{1}{R_\lambda} \sum_k \Delta a_k \xi_k, \\ \Delta \vartheta(\mathbf{r}) &= \sum_j \sum_k \Delta B_{jk} \xi_j \xi_k + \frac{1}{Pe} \sum_k \Delta b_k \xi_k\end{aligned}\tag{40}$$

Conversely, the second and third statistical moments of  $\Delta u_r$  and  $\Delta \vartheta$  are coupled via the energy cascade mechanism, in accordance with Eqs. (5) and (4). By substituting the decompositions (40) into Eqs. (5) and taking into account that  $|\langle \xi_k^3 \rangle| \gg \langle \xi_k^n \rangle, \forall n \neq 3$ , it is found that Eqs. (5) are identically satisfied by the quasi-PDF:

$$\hat{\delta}(\xi_k) = \delta_e(\xi_k) - \frac{\langle \xi_k^3 \rangle}{3!} \delta^{(3)}(\xi_k)\tag{41}$$

if and only if the following condition holds:

$$\langle \xi_k^3 \rangle = \frac{C}{R_\lambda^3}\tag{42}$$

where  $C$  is an arbitrary constant, and provided that:

$$\frac{\sum_k \Delta A_{kk} \Delta B_{kk}^2}{\sum_k \Delta a_{kk} \Delta b_{kk}^2} \sim \left( \frac{1}{Pr} \right)^2\tag{43}$$

Within the theoretical framework of the Fisher parsimony principle, these results provide robust confirmation that Eqs. (41) and (42) constitute the necessary and sufficient conditions for the velocity and temperature gradients,  $\partial u_r / \partial r$  and  $\partial \vartheta / \partial r$  as defined through Eqs.(40), to exhibit constant, non-zero negative skewness values in strict accordance with Eqs. (5). Notably, these

equations represent quasi-PDFs of non-observable quantities whose analytical structure accounts for the energy flux of the cascade while rigorously preserving the mean kinetic energy of the system.

## 5. Statistics of velocity and temperature difference

To evaluate the statistics of  $\Delta u_r$  and  $\Delta \vartheta$ , the matrices  $\Delta A_{jk}$  and  $\Delta B_{jk}$  in Eq. (40), are first decomposed into their respective symmetric parts  $(S_{ujk}, S_{\theta jk})$ , associated with the local strain and dissipation, and antisymmetric parts  $(\Omega_{ujk}, \Omega_{\theta jk})$ , associated with the local vorticity.

$$\begin{aligned}\Delta A_{jk} &= \sum_{i=1}^3 \left( A_{jk}^{(i)}(\mathbf{x} + \mathbf{r}) - A_{jk}^{(i)}(\mathbf{x}) \right) \frac{r_i}{r} \equiv S_{ujk} + \Omega_{ujk} \\ \Delta a_k &= \sum_{i=1}^3 \left( a_k^{(i)}(\mathbf{x} + \mathbf{r}) - a_k^{(i)}(\mathbf{x}) \right) \frac{r_i}{r}\end{aligned}\tag{44}$$

$$\Delta B_{jk} = B_{jk}(\mathbf{x} + \mathbf{r}) - B_{jk}(\mathbf{x}) \equiv S_{\theta jk} + \Omega_{\theta jk}$$

$$\Delta b_k = b_k(\mathbf{x} + \mathbf{r}) - b_k(\mathbf{x})$$

This decomposition allows us to trace the emergence of non-Gaussian tails directly to the non-linear interaction of bifurcation modes at the scales of the energy cascade. The terms involving  $\Omega_{ujk}$  and  $\Omega_{\theta jk}$  yield a null contribution to Eqs. (40). Consequently,  $S_{ujk}$  and  $S_{\theta jk}$  are decomposed into their spectral diagonal components and a residual coupling matrix by applying a spectral shift to the main diagonal:

$$S_{Xjk} = \Lambda_{Xjk}^+ - \Lambda_{Xjk}^- + R_{Xjk}, \quad X = u, \theta\tag{45}$$

where  $\Lambda_{Xjk}^+$  and  $-\Lambda_{Xjk}^-$  denote diagonal matrices whose non-zero entries correspond to the positive and non-positive eigenvalues of  $S_{Xjk}$ , respectively, while  $R_{Xjk}$  represents the residual matrices. The latter satisfy the Gerschgorin circle theorem, according to which the absolute value of the diagonal residual  $|R_{Xii}|$  is bounded by the sum of the absolute values of the off-diagonal elements in the corresponding row of  $\mathbf{R}_X$ .

Accordingly, the velocity and temperature increments can be expressed as:

$$\Delta u_r(\mathbf{r}) = \sum_{jk} (\Lambda_{ujk}^+ - \Lambda_{ujk}^-) \xi_j \xi_k + \sum_{jk} R_{ujk} \xi_j \xi_k + \frac{1}{R_\lambda} \sum_k \Delta a_k \xi_k, \quad (46)$$

$$\Delta \vartheta(\mathbf{r}) = \sum_{jk} (\Lambda_{\theta jk}^+ - \Lambda_{\theta jk}^-) \xi_j \xi_k + \sum_{jk} R_{\theta jk} \xi_j \xi_k + \frac{1}{Pe} \sum_k \Delta b_k \xi_k$$

Consequently, the centered fluctuations of  $\Delta u_r$  and  $\Delta \vartheta$  are reformulated as functions of the variables  $\eta_X$ ,  $\eta_{X+}$ , and  $\eta_{X-}$  (for  $X = u, \theta$ ):

$$\Delta u_r = \eta_u + (\eta_{u+}^2 - \langle \eta_{u+}^2 \rangle) - (\eta_{u-}^2 - \langle \eta_{u-}^2 \rangle), \quad (47)$$

$$\Delta \vartheta = \eta_\theta + (\eta_{\theta+}^2 - \langle \eta_{\theta+}^2 \rangle) - (\eta_{\theta-}^2 - \langle \eta_{\theta-}^2 \rangle),$$

where these variables are defined as follows:

$$\eta_{X+} = \sum_k (\Lambda_{Xkk}^+)^{1/2} \xi_k, \quad \eta_{X-} = \sum_k (\Lambda_{Xkk}^-)^{1/2} \xi_k, \quad X = u, \theta, \quad (48)$$

$$\eta_u = \frac{1}{R_\lambda} \sum_i \Delta a_i \xi_i + \sum_{jk} F_{ujk} \xi_j \xi_k, \quad (49)$$

$$\eta_\theta = \frac{1}{Pe} \sum_i \Delta b_i \xi_i + \sum_{jk} F_{\theta jk} \xi_j \xi_k,$$

with

$$F_{Xjk} = R_{Xjk} + (\Lambda_{Xjj}^- \Lambda_{Xkk}^-)^{1/2} - (\Lambda_{Xjj}^+ \Lambda_{Xkk}^+)^{1/2}, \quad X = u, \theta \quad (50)$$

We now demonstrate that  $\eta_X$ ,  $\eta_{X-}$ , and  $\eta_{X+}$  asymptotically approach uncorrelated Gaussian variables. Indeed, as per Eq. (48),  $\eta_{X+}$  and  $\eta_{X-}$  are sums of terms derived from two distinct sets of uncorrelated stochastic variables. Thus,  $\eta_{X+}$  and  $\eta_{X-}$  emerge as centered uncorrelated stochastic variables, such that  $\langle \eta_{X+} \rangle = \langle \eta_{X-} \rangle = 0$ . Furthermore, since the  $\xi_k$  are statistically independent, even if they are described by quasi-PDFs, the application of the Central Limit Theorem (CLT) to Eq. (48) ensures that both  $\eta_{X+}$  and  $\eta_{X-}$  converge to centered Gaussian random variables.

Regarding  $\eta_X$ , the following considerations apply: the first terms on the right-hand side (RHS) of Eqs. (49) are sums of uncorrelated variables described by quasi-PDFs, where both  $\Delta a_i$  and  $\Delta b_i$  satisfy the Lindeberg condition. The second terms are quadratic forms where, due to the structure of the matrices  $\mathbf{F}_X$  in Eqs. (50) and the fact that  $\mathbf{R}_X$  satisfies the Gerschgorin theorem, the spectral radii of  $\mathbf{F}_X$  are negligible compared to their corresponding Frobenius norms. This constitutes a necessary and sufficient condition for  $\eta_X$  to be distributed according to a Gaussian PDF [61].

Hence, the statistics of  $\Delta u_r$  and  $\Delta \vartheta$  can be reduced to structure functions of the independent centered Gaussian stochastic variables  $\zeta_X$ ,  $\zeta_{X+}$ , and  $\zeta_{X-}$ , obtained by normalizing  $\eta_X$ ,  $\eta_{X+}$ , and  $\eta_{X-}$ , respectively, such that  $\langle \zeta_X^2 \rangle = \langle \zeta_{X+}^2 \rangle = \langle \zeta_{X-}^2 \rangle = 1$ :

$$\Delta u_r = L_u \zeta_u + S_u^+ (\zeta_{u+}^2 - 1) - S_u^- (\zeta_{u-}^2 - 1), \quad (51)$$

$$\Delta \vartheta = L_\theta \zeta_\theta + S_\theta^+ (\zeta_{\theta+}^2 - 1) - S_\theta^- (\zeta_{\theta-}^2 - 1),$$

where  $L_X$ ,  $S_X^+$ , and  $S_X^-$  are normalization coefficients introduced to ensure that  $\zeta_X$ ,  $\zeta_{X+}$ , and  $\zeta_{X-}$  possess unit standard deviation. Thus:

$$L_u \zeta_u = \sum_{ij} F_{uij} \xi_i \xi_j + \frac{1}{R_\lambda} \sum_k \Delta a_k \xi_k, \quad (52)$$

$$L_\theta \zeta_\theta = \sum_{ij} F_{\theta ij} \xi_i \xi_j + \frac{1}{Pe} \sum_k \Delta b_k \xi_k,$$

where the  $r$ -dependent parameters  $L_X$ ,  $S_X^-$ , and  $S_X^+$  remain to be determined.

In this regard, it is noteworthy that, according to Fisher [22], in a regime of fully developed isotropic turbulence within an infinite domain, the number of parameters required to describe the statistics of  $\Delta u_r$  and  $\Delta \vartheta$  should be the minimum compatible with the prescribed physical quantities defining the state of motion (e.g., average kinetic energy, temperature standard deviation, and correlation functions). Furthermore, the evolution equation for the velocity pair correlation  $f$  [3] requires knowledge of the third-order correlations  $k$ . Consequently, within the framework of estimating the evolution of  $f$  in fully developed homogeneous isotropic turbulence, the knowledge of  $f$  and  $k$  alone is considered necessary and sufficient to determine the statistics of  $\Delta u_r$ . This implies that  $S_u^+$  is proportional to  $S_u^-$  through a quantity independent of  $r$ , namely:

$$S_u^+(r) = \chi S_u^-(r) \equiv \chi S_u(r) \quad (53)$$

where  $\chi < 1$  is a function of  $R_\lambda$  representing the skewness of  $\Delta u_r$ . Accordingly,  $S_u$  and  $L_u$  are determined as functions of  $f$  and  $k$  once  $\chi = \chi(Re)$  is identified. Regarding the temperature difference, turbulence isotropy dic-

tates that the skewness of  $\Delta\vartheta$  must vanish, yielding:

$$S_\theta^+(r) = S_\theta^-(r) \equiv S_\theta(r) \quad (54)$$

The structure functions for  $\Delta u_r$  and  $\Delta\vartheta$  thus read:

$$\Delta u_r = L_u \zeta_u + S_u (\chi (\zeta_{u+}^2 - 1) - (\zeta_{u-}^2 - 1)), \quad (55)$$

$$\Delta\vartheta = L_\theta \zeta_\theta + S_\theta (\zeta_{\theta+}^2 - \zeta_{\theta-}^2),$$

Finally, invoking the principle of the minimum number of parameters, the ratio  $\Psi_\theta(r) \equiv S_\theta/L_\theta$  is assumed to be proportional to  $\Psi_u(r) \equiv S_u/L_u$  via a coefficient solely dependent on the Prandtl number:

$$\Psi_\theta(r) = \sigma(Pr)\Psi_u(r) \quad (56)$$

where  $\sigma(Pr)$  is a function to be determined.

At this stage of the analysis, we demonstrate that in the regime of fully developed turbulence,  $L_u$  and  $L_\theta$  are functions of  $R_\lambda$  and  $Pe$ , respectively, scaling as  $L_u \propto R_\lambda^{-1/2}$  and  $L_\theta \propto Pe^{-1/2}$ . Indeed, from Eq. (52), we obtain:

$$L_u^2 = \sum_{ijkl} F_{uij} F_{ukl} \langle \xi_i \xi_j \xi_k \xi_l \rangle + \frac{2}{R_\lambda} \sum_k F_{ukk} \Delta a_{uk} \langle \xi_k^3 \rangle + \frac{1}{R_\lambda^2} \sum_k \Delta a_k^2 \langle \xi_k^2 \rangle, \quad (57)$$

$$L_\theta^2 = \sum_{ijkl} F_{\theta ij} F_{\theta kl} \langle \xi_i \xi_j \xi_k \xi_l \rangle + \frac{2}{Pe} \sum_k F_{\theta kk} \Delta b_k \langle \xi_k^3 \rangle + \frac{1}{Pe^2} \sum_k \Delta b_k^2 \langle \xi_k^2 \rangle,$$

Since  $\xi_k$  represent bifurcation modes described by Gram–Charlier quasi-PDFs, the condition  $|\langle \xi_k^3 \rangle| \gg 1$ ,  $\langle \xi_i \xi_j \xi_k \xi_l \rangle$  holds. Consequently, the first and third terms on the right-hand side of Eq. (57) become negligible, implying

that  $L_u$  and  $L_\theta$  admit the following functional forms:

$$L_u = \frac{M_u(r)}{\sqrt{R_\lambda}},$$

$$L_\theta = \frac{M_\theta(r)}{\sqrt{Pe}}.$$
(58)

where  $M_u(r)$  and  $M_\theta(r)$  are  $r$ -dependent functions that do not exhibit direct dependence on  $R_\lambda$  and  $Pe$ .

Hence, the dimensionless increments  $\Delta u_r$  and  $\Delta \vartheta$ , normalized by their respective standard deviations, are expressed as functions of  $R_\lambda$  and  $Pe$ :

$$\frac{\Delta u_r}{\sqrt{\langle (\Delta u_r)^2 \rangle}} = \frac{\zeta_u + \Psi_u(\chi(\zeta_{u+}^2 - 1) - (\zeta_{u-}^2 - 1))}{\sqrt{1 + 2\Psi_u^2(1 + \chi^2)}},$$

$$\Psi_u(r) = \frac{S_u(r)}{L_u(r)} = \Phi(r)\sqrt{R_\lambda},$$

$$\frac{\Delta \vartheta}{\sqrt{\langle (\Delta \vartheta)^2 \rangle}} = \frac{\zeta_\theta + \Psi_\theta(\zeta_{\theta+}^2 - \zeta_{\theta-}^2)}{\sqrt{1 + 4\Psi_\theta^2}},$$

$$\Psi_\theta(r) = \frac{S_\theta(r)}{L_\theta(r)} = \Phi(r)\sqrt{Pe}$$
(59)

which identifies the relationship  $\sigma = \sqrt{Pr}$ . Eqs. (59) define the specific structure functions governing the statistics of  $\Delta u_r$  and  $\Delta \vartheta$ .

It is noteworthy that the term involving  $\Psi_u$  accounts for the intermittency of  $\Delta u_r$ . Furthermore, according to Eqs. (29) and (31), we have  $\Psi_u(0) \sim (u/u_k)^2(\ell_k/\lambda_T)$ , where  $u$  and  $u_k$  denote the velocity standard deviation and the Kolmogorov velocity, respectively, while  $\ell_k$  and  $\lambda_T$  represent the Kolmogorov scale and the Taylor microscale.

Remarkably, the present approach, by leveraging non-observable bifurcation modes and their corresponding quasi-PDFs, recovers the Kolmogorov scaling law, which states that  $u/u_k \sim (u/u_k)^2(\ell_k/\lambda_T) \sim \sqrt{R_\lambda}$ . This suggests that the non-observability of bifurcation modes constitutes the fundamental conceptual link between the intermittency of  $\Delta u_r$  and the Kolmogorov law. Without invoking such non-observability, while intermittency could still be identified, the derivation of the Kolmogorov law would remain inaccessible.

Now, assuming  $\chi = \chi(R_\lambda)$  is known,  $L_u$  and  $S_u$  can be expressed as functions of  $\langle \Delta u_r^2 \rangle$  and  $\langle \Delta u_r^3 \rangle$ , where the latter is determined by adopting the proposed closure (3). In fact,  $L_u$  and  $S_u$  are related to these moments through Eq. (55):

$$\langle (\Delta u_r)^3 \rangle = 6u^3k = 8S_u^3(\chi^3 - 1), \quad (60)$$

$$\langle (\Delta u_r)^2 \rangle = 2u^2(1 - f) = L_u^2 + 2S_u^2(\chi^2 + 1),$$

Consequently,  $L_u$ ,  $S_u$ , and  $\Phi$  are expressed in terms of  $f(r)$  and  $k(r)$  as follows:

$$S_u(r) = \left( \frac{3/4}{\chi^3 - 1} \right)^{1/3} u k(r)^{1/3},$$

$$L_u(r) = \sqrt{2} u \sqrt{1 - f(r) - (1 + \chi^2) \left( \frac{3/4}{\chi^3 - 1} \right)^{2/3} k(r)^{2/3}}, \quad (61)$$

$$\Phi = \frac{S_u}{L_u} \frac{1}{\sqrt{R_\lambda}}$$

In the expression for  $L_u(r)$  in Eqs. (61), the argument of the square root

must be strictly positive, leading to the following implicit condition for  $\chi$ :

$$\frac{1 + \chi^2}{(\chi^3 - 1)^{2/3}} \leq \frac{1}{2} \left( \frac{56}{3} \right)^{2/3} \quad (62)$$

incorporating the proposed closure (3). Solving inequality (62) for  $\chi$  yields the upper bound:

$$\chi \leq \chi_\infty = 0.8659... \quad (63)$$

Regarding the temperature difference, we have:

$$\frac{\langle (\Delta u_r)^2 \rangle}{\langle (\Delta \vartheta)^2 \rangle} \equiv \frac{u^2}{\theta^2} \frac{1 - f}{1 - f_\theta} = \frac{L_u^2}{L_\theta^2} \frac{1 + 2\Psi_u^2(1 + \chi^2)}{1 + 4\Psi_\theta^2} \quad (64)$$

Thus, Eq. (64) allows for the calculation of  $L_\theta$  in terms of the other quantities:

$$L_\theta = L_u \frac{\theta}{u} \sqrt{\frac{1 - f_\theta}{1 - f}} \sqrt{\frac{1 + 2\Phi^2 R_\lambda (1 + \chi^2)}{1 + 4\Phi^2 Pe}} \quad (65)$$

In Eqs. (65) and (61), the function  $\chi = \chi(R_\lambda)$  must be identified; furthermore,  $\Phi(r)$  depends on the specific profile of  $f(r)$ . Due to the constancy of  $H_u^{(3)}(0)$  and according to the Fisher principle,  $\Phi(0)$  is assumed to be a constant independent of  $R_\lambda$ .

The PDFs of  $\Delta u_r$  and  $\Delta \vartheta$  are formally derived via the Frobenius–Perron equation [62], considering that  $\zeta_X$ ,  $\zeta_{X-}$ , and  $\zeta_{X+}$  are independent, identically distributed centered Gaussian variables such that  $\langle \zeta_X^2 \rangle = \langle \zeta_{X-}^2 \rangle = \langle \zeta_{X+}^2 \rangle = 1$  for  $X = u, \theta$ :

$$F_u(\Delta u_r') = \int_{\zeta} \int_{\zeta_-} \int_{\zeta_+} P(\zeta, \zeta_-, \zeta_+) \delta(\Delta u_r' - \Delta u_r(\zeta, \zeta_-, \zeta_+)) d\zeta d\zeta_- d\zeta_+, \quad (66)$$

$$F_\theta(\Delta \vartheta') = \int_{\zeta} \int_{\zeta_-} \int_{\zeta_+} P(\zeta, \zeta_-, \zeta_+) \delta(\Delta \vartheta' - \Delta \vartheta(\zeta, \zeta_-, \zeta_+)) d\zeta d\zeta_- d\zeta_+,$$

where  $\delta$  is the Dirac delta function and  $P(\zeta, \zeta_-, \zeta_+)$  is the trivariate Gaussian PDF:

$$P(\zeta, \zeta_-, \zeta_+) = \frac{1}{\sqrt{(2\pi)^3}} \exp\left(-\frac{\zeta^2 + \zeta_-^2 + \zeta_+^2}{2}\right), \quad (67)$$

with  $\Delta u_r(\zeta, \zeta_-, \zeta_+)$  and  $\Delta \vartheta(\zeta, \zeta_-, \zeta_+)$  determined by Eqs. (59).

In essence, the statistics of  $\Delta u_r$  and  $\Delta \vartheta$  can be inferred from the proposed statistical decomposition (35), which accounts for bifurcation effects in isotropic turbulence. This results in non-Gaussian statistics where the absolute values of the dimensionless moments increase with  $R_\lambda$  and  $Pe$ . Specifically, the dimensionless statistical moments are calculated as:

$$H_u^{(n)} \equiv \frac{\langle (\Delta u_r)^n \rangle}{\langle (\Delta u_r)^2 \rangle^{n/2}} = \frac{1}{(1 + 2(1 + \chi^2)\Psi_u^2)^{n/2}} \sum_{k=0}^n \binom{n}{k} \Psi_u^k \langle \zeta_u^{n-k} \rangle \langle (\chi(\zeta_{u+}^2 - 1) - (\zeta_{u-}^2 - 1))^k \rangle, \quad (68)$$

$$H_\theta^{(n)} \equiv \frac{\langle (\Delta \vartheta)^n \rangle}{\langle (\Delta \vartheta)^2 \rangle^{n/2}} = \frac{1}{(1 + 4\Psi_\theta^2)^{n/2}} \sum_{k=0}^n \binom{n}{k} \Psi_\theta^k \langle \zeta_\theta^{n-k} \rangle \langle (\zeta_{\theta+}^2 - \zeta_{\theta-}^2)^k \rangle,$$

where  $\Phi(0)$  and  $\chi = \chi(R_\lambda)$  remain to be identified. To this end, we first analyze the statistics of  $\partial u_r / \partial r$ , which, according to the proposed Lyapunov analysis, exhibits a constant skewness  $H_u^{(3)}(0) = -3/7$ . From Eqs. (68), we obtain:

$$H_u^{(3)}(r) = \frac{8\Psi_u^3(\chi^3 - 1)}{(1 + 2\Psi_u^2(1 + \chi^2))^{3/2}} \quad (69)$$

and taking the limit  $r \rightarrow 0$ :

$$H_u^{(3)}(0) = \frac{8\Psi_u^3(0)(\chi^3 - 1)}{(1 + 2\Psi_u^2(0)(1 + \chi^2))^{3/2}} \quad (70)$$

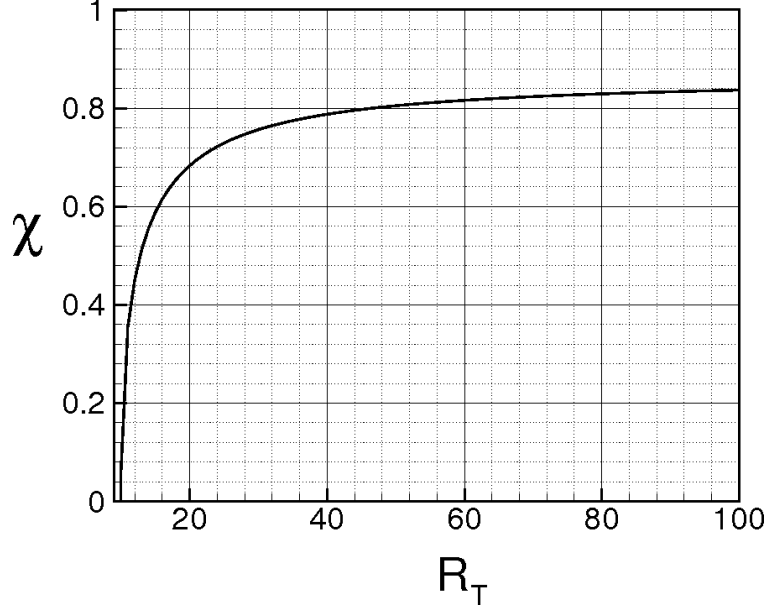


Figure 1: Characteristic Function  $\chi=\chi(R_\lambda)$

Accordingly,  $\chi = \chi(R_\lambda)$  is implicitly defined as a function of  $\Phi(0)\sqrt{R_\lambda}$ . Eq. (70) shows that  $\chi(R_\lambda)$  is a monotonically increasing function of  $R_\lambda$ , which, for  $H_u^{(3)}(0) = -3/7$ , reaches the limit  $\chi_\infty = 0.8659\dots$  as  $R_\lambda \rightarrow \infty$ . For sufficiently small  $R_\lambda$ ,  $\chi(R_\lambda)$  may become negative. However, in fully developed turbulence, the PDF of  $\partial u_r/\partial r$  must exhibit non-Gaussian tails as  $\partial u_r/\partial r \rightarrow \pm\infty$ , requiring  $\chi$  to be positive. Thus, the limit  $\chi = 0$  is assumed to occur at  $R_\lambda = R_\lambda^* = 10$ , representing the threshold for homogeneous isotropic turbulence. This allows for the identification of  $\Phi(0)$  via Eq. (70):

$$\Phi(0) = \frac{1}{\sqrt{R_\lambda^*}} \sqrt{\frac{H_{u0}^{(3)2/3}}{4 - 2H_{u0}^{(3)2/3}}} = 0.1409\dots \quad (71)$$

The resulting implicit variation law  $\chi = \chi(R_\lambda)$  is illustrated in Fig. 1. To validate the value of  $\Phi(0)$  calculated in Eq. (71), we consider that the order

of magnitude scales as  $\Phi(0) \sim (u/u_K)^2(\ell_K/\lambda_T)$ . Given that:

$$\frac{\lambda_T}{\ell_K} = 15^{1/4} \sqrt{R_\lambda}, \quad \frac{u_K \ell_K}{\nu} = 1, \quad R_\lambda = \frac{u \lambda_T}{\nu} \quad (72)$$

it follows that:

$$\Phi(0) \sim \left(\frac{u}{u_K}\right)^2 \frac{\ell_K}{\lambda_T} = \frac{1}{\sqrt{15\sqrt{15}}} \simeq 0.1312 \quad (73)$$

The value of  $\Phi(0) = 0.1409$  obtained in Eq. (71) via  $H_{u0}^{(3)}$  and  $R_\lambda^*$  is in close agreement with the aforementioned estimate. This consistency indicates that the proposed closure of the von Kármán–Howarth equation [26], the prediction of  $R_\lambda^*$  established in the previous section, and the present analysis provide a robust framework for describing the link between the Kolmogorov scaling law and intermittency.

We conclude this section with the following fundamental considerations. The current approach, by leveraging non-observable bifurcation modes and their corresponding quasi-PDFs, successfully recovers the Kolmogorov scaling law, which dictates that  $u/u_k \sim (u/u_k)^2(\ell_k/\lambda_T) \sim \sqrt{R_\lambda}$ . This result suggests that the non-observability of bifurcation modes constitutes the primary conceptual bridge connecting the intermittency of  $\Delta u_r$  to the Kolmogorov law. While intermittency might be identified through other means, the rigorous derivation of the Kolmogorov law would remain inaccessible without invoking the principle of non-observability of these modes.

## 6. Analytical Expressions for Velocity and Temperature Increment Probability Density Functions

Based on the preceding analysis, this section derives the analytical structure of the PDFs  $F_u(\Delta u_r)$  and  $F_\theta(\Delta \vartheta)$ . These distributions are obtained by

combining the structural relations for  $\Delta u_r$  and  $\Delta \vartheta$  in terms of reduced Gaussian variables [Eq. (59)] with the Frobenius–Perron equations (66) and (67). In the general case, the PDFs  $F_u(\Delta u_r)$  and  $F_\theta(\Delta \vartheta)$  do not admit a simple closed-form expression; however, they can be expressed as the convolution of a Gaussian PDF and a modified Bessel function of the second kind,  $K_0$

$$K_0(x) = \int_0^\infty \frac{\cos(xt)}{\sqrt{1+t^2}} dt \quad (74)$$

Consistent with Eqs. (59), we consider dimensionless velocity and temperature increments characterized by unit standard deviation. To this end, we introduce the variable  $s$ , representing either  $\Delta u_r$  or  $\Delta \vartheta$  depending on the context, defined as:

$$s = \frac{\Delta u_r}{\sqrt{\langle (\Delta u_r)^2 \rangle}} = \frac{\zeta_u + \Psi_u[\chi(\zeta_{u+}^2 - 1) - (\zeta_{u-}^2 - 1)]}{\sqrt{1 + 2\Psi_u^2(1 + \chi^2)}}, \quad (75)$$

$$s = \frac{\Delta \vartheta}{\sqrt{\langle (\Delta \vartheta)^2 \rangle}} = \frac{\zeta_\theta + \Psi_\theta(\zeta_{\theta+}^2 - \zeta_{\theta-}^2)}{\sqrt{1 + 4\Psi_\theta^2}},$$

By applying Eqs. (66), (67), and (75), the velocity increment PDF,  $F_u(s)$ , is given by:

$$F_u(s) = \int_{-\infty}^{\infty} \frac{1}{\sqrt{2\pi}\alpha_u} e^{-\frac{(s-\zeta)^2}{2\alpha_u^2}} Q_u(\zeta) d\zeta,$$

$$Q_u(\zeta) = \frac{1}{2\pi\sqrt{\beta_1\beta_2}} \exp\left(\frac{\Delta\beta}{4\beta_1\beta_2}(\zeta + \Delta\beta)\right) K_0\left(\frac{\beta_1 + \beta_2}{4\beta_1\beta_2}|\zeta + \Delta\beta|\right), \quad (76)$$

$$\alpha_u = \frac{1}{\sqrt{1 + 2\Psi_u^2(1 + \chi^2)}}, \quad \beta_1 = \chi\Psi_u\alpha_u, \quad \beta_2 = \Psi_u\alpha_u, \quad \Delta\beta = \beta_1 - \beta_2$$

This function exhibits a pronounced asymmetry, with a corresponding skewness value arising from the turbulent energy cascade. Conversely, the tem-

perature increment PDF remains even due to local isotropy:

$$F_\theta(s) = \int_{-\infty}^{\infty} \frac{1}{\sqrt{2\pi\alpha_\theta}} e^{-\frac{(s-\zeta)^2}{2\alpha_\theta^2}} Q_\theta(\zeta) d\zeta,$$

$$Q_\theta(\zeta) = \frac{1}{2\pi\beta} K_0\left(\frac{1}{2\beta}|\zeta|\right), \quad (77)$$

$$\alpha_\theta = \frac{1}{\sqrt{1+4\Psi_\theta^2}}, \quad \beta = \Psi_\theta \alpha_\theta,$$

For the detailed mathematical derivation showing that the convolution of a Gaussian kernel with  $K_0$  arises from the distribution of second-order moment statistics, the reader is referred to the seminal work of Wishart and Bartlett [63]. The convolution structure given by Eqs. (76) and (77) between Gaussian kernel and  $K_0$  is consistent with the general framework for velocity probability density functions proposed by Castaing et al. [64] and specifically discussed for passive scalars and velocity increments in [65, 66].

The convolutions (76) and (77) reveal that the linear-Gaussian term in Eqs. (59), which stems from fluid diffusivity (viscosity or thermal conductivity), acts as a smoothing and regularizing agent for the PDFs near the origin. In the absence of this term, a singular peak would emerge at the origin for the temperature increment PDF and near the origin for the velocity increment PDF. Thus, the Bessel function captures the effects of intermittency, while the Gaussian kernel tends to regularize this intermittency, particularly at moderate Reynolds numbers. While the skewness remains constant, the degree of intermittency increases with both the Reynolds and Peclet numbers, reaching its maximum in the limits  $R_\lambda \rightarrow \infty$  and  $Pe \rightarrow \infty$ .

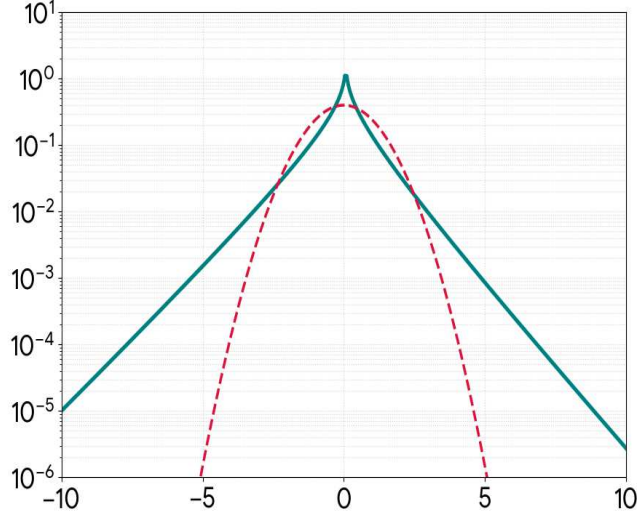


Figure 2: Probability Density Function of  $s = \partial u_r / \partial r / \sqrt{\langle (\partial u_r / \partial r)^2 \rangle}$  for  $R_\lambda \rightarrow \infty$  in comparison with a Gaussian PDF.

In these asymptotic limits ( $R_\lambda \rightarrow \infty$  and  $Pe \rightarrow \infty$ ), both PDFs admit exact analytical solutions. These forms are obtained as  $\Psi_u \rightarrow \infty$  and  $\Psi_\theta \rightarrow \infty$  using Eqs. (66) and (67). Accordingly,  $\alpha_u \rightarrow 0$ ,  $\alpha_\theta \rightarrow 0$ , the Gaussian kernels tend to Dirac delta, and the velocity increment PDF converges to:

$$F_u(s) = \frac{1}{2\pi\sqrt{\beta_1\beta_2}} \exp\left(\frac{\Delta\beta}{4\beta_1\beta_2}(s + \Delta\beta)\right) K_0\left(\frac{\beta_1 + \beta_2}{4\beta_1\beta_2}|s + \Delta\beta|\right) \quad (78)$$

with the parameters defined as:

$$\beta_1 = \frac{\chi_\infty}{\sqrt{2(1 + \chi_\infty^2)}}, \quad \beta_2 = \frac{1}{\sqrt{2(1 + \chi_\infty^2)}}, \quad \Delta\beta = \beta_1 - \beta_2, \quad \chi_\infty \approx 0.8659, \quad (79)$$

whereas the temperature increment PDF becomes purely symmetric and is directly represented by the  $K_0$  function:

$$F_\theta(s) = \frac{1}{\pi} K_0(|s|) \quad (80)$$

Figures 2 and 3 illustrate the behavior of both PDFs under these conditions, compared to Gaussian distributions with the same standard deviation. In

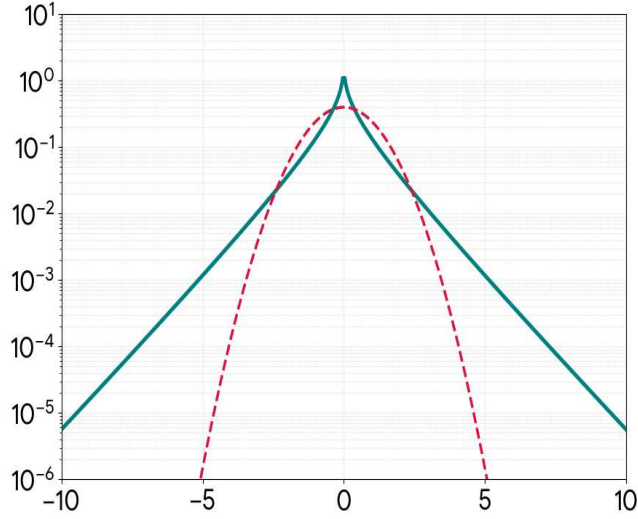


Figure 3: Probability Density Function of  $s = \partial\vartheta/\partial r / \sqrt{\langle(\partial\vartheta/\partial r)^2\rangle}$  for  $Pe \rightarrow \infty$  compared with a Gaussian PDF.

this regime, intermittency is maximized, as evidenced by the heavy tails dictated by the asymptotic decay of the modified Bessel function. Notably, the velocity increment PDF maintains a constant skewness of  $-3/7$ , which is invariant with respect to the Reynolds number. Furthermore, both PDFs exhibit a singular peak: for the temperature increment, symmetry induced by isotropy locates this singularity at the origin, whereas for the velocity increment, the singularity is shifted to  $s = \beta_2 - \beta_1 \approx 0.0717$  due to the inherent asymmetry of the kinetic energy cascade. Consequently, the asymptotic decay for both PDFs follows the form  $\sim \exp(-|s|) / \sqrt{|s|}$ .

We conclude this section by observing that the convolutions (76) and (77) have been derived from the analytical expressions of the previously defined velocity and temperature fluctuations, obtained in turn through the Navier–Stokes and heat equations.

## 7. Results and Discussion

In this section, we present the results obtained from the current analysis, providing a comparative evaluation with established data from the literature. As demonstrated in Ref. [23], the statistical framework defined by Eqs. (66) and (68) exhibits close agreement with the experimental evidence reported in Refs. [67, 68]. In those studies, the PDF of the longitudinal velocity gradient  $\partial u_r/\partial r$  and its higher-order moments were measured using low-temperature helium gas within a closed cell between counter-rotating cylinders. Although those experiments involved wall-bounded flows, the measured velocity difference PDFs are remarkably consistent with the present theoretical results (Eqs. (66) and (68)). Despite a slightly non-monotonic evolution of the fourth and sixth moments ( $H_u^{(4)}(0)$  and  $H_u^{(6)}(0)$ ) observed in [67, 68], the dimensionless statistical moments of  $\partial u_r/\partial r$  follow the same trends and order of magnitude as those calculated via Eqs. (68). In particular, the PDFs derived from the present analysis successfully capture the non-Gaussian tails observed experimentally.

In Fig. 4 a), b) and c) the normalized PDFs of  $\partial u_r/\partial r$ , computed using Eqs. (66) and (59), are presented in terms of the standardized variable  $s$ :

$$s = \frac{\partial u_r/\partial r}{\sqrt{\langle(\partial u_r/\partial r)^2\rangle}} \quad (81)$$

such that the standard deviation is unity. The results in Fig. 4a correspond to  $R_\lambda = 15, 30$ , and  $60$ , while Figs. 4b and 4c report the PDFs for  $R_\lambda$  ranging from  $255$  to  $1553$ . Fig. 4c, in particular, highlights the PDF tails in the range  $5 < s < 8$ . According to the present analysis, the PDF tails broaden with the Reynolds number in the interval  $10 < R_\lambda < 700$ , while beyond  $R_\lambda >$

700, the variations become increasingly marginal. The comparison with the results of [67] demonstrates that Fig. 4c yields PDF magnitudes and average slopes in good agreement with experimental data, particularly in the far-tail region ( $s > 5$ ). It should be noted that the slight discrepancies and non-monotonic trends in the experimental data may arise from the departure from perfect isotropy inherent in wall-bounded flows, where boundary effects can significantly influence the velocity field near the probe. More in detail, Table 1 shows the variations of the dimensionless statistical moments of  $\partial u_r / \partial r$  in function of  $R_\lambda$  following Eq. (68). The scaling exponents  $\zeta_V(n)$  associated with the  $n$ -th order moments of  $\Delta u_r$ , defined as:

$$\langle (\Delta u_r)^n \rangle \approx A_n r^{\zeta_V(n)}, \quad (82)$$

were determined through post-processing of the results obtained in Refs. [23, 32] using Eq. (59) via an optimization procedure. First, the statistical moments of  $\Delta u_r$  are calculated as functions of  $r$  (Fig. 5). Subsequently, the exponents  $\zeta_V(n)$  are identified through a least-squares method applied to the following objective function:

$$J_n(\zeta_V(n), A_n) \equiv \int_{\hat{r}_1}^{\hat{r}_2} (\langle (\Delta u_r)^n \rangle - A_n r^{\zeta_V(n)})^2 dr = \min, \quad n = 1, 2, \dots \quad (83)$$

where the integration limits, in the inertial range, are set to  $\hat{r}_1 = 0.1$  and  $\hat{r}_2$  is chosen such that  $\zeta_V(3) = 1$  is satisfied. The resulting exponents are displayed in Fig. 5 and compared with Kolmogorov's K41 [2] and K62 [10] theories, as well as the She-Leveque model [69]. For  $n < 4$ , the exponents follow the classical  $\zeta_V(n) \approx n/3$  scaling. For higher orders, however, the nonlinear terms in Eq. (59) induce a distinct multiscaling behavior. The

calculated exponents show excellent agreement with the She–Leveque curve, being only slightly higher for  $n > 8$ .

Regarding the temperature increment statistics, Fig. 6 illustrates the distribution function of  $\partial\vartheta/\partial r$  in terms of the dimensionless variable:

$$s = \frac{\partial\vartheta/\partial r}{\sqrt{\langle(\partial\vartheta/\partial r)^2\rangle}} \quad (84)$$

as computed via Eqs. (66) and (59) for various values of  $\Psi_\theta$ . To quantify the intermittency of the temperature field, the flatness  $H_\theta^{(4)}$  and hyperflatness  $H_\theta^{(6)}$ , defined as:

$$H_\theta^{(4)} = \frac{\langle s^4 \rangle}{\langle s^2 \rangle^2}, \quad H_\theta^{(6)} = \frac{\langle s^6 \rangle}{\langle s^2 \rangle^3} \quad (85)$$

are plotted in Fig. 6 against  $\Psi_\theta$ . For  $\Psi_\theta = 0$ , the PDF is Gaussian ( $H_\theta^{(4)} = 3$ ,  $H_\theta^{(6)} = 15$ ). As  $\Psi_\theta$  increases, the nonlinear contributions from  $\zeta_{\theta-}$  and  $\zeta_{\theta+}$  drive a significant increase in these moments, with  $H_\theta^{(4)}$  and  $H_\theta^{(6)}$  asymptotically approaching 9 and 225, respectively, as  $\Psi_\theta \rightarrow \infty$ .

Finally, the statistical properties of the temperature dissipation rate, defined as:

$$\varphi = 2\kappa\nabla\vartheta \cdot \nabla\vartheta, \quad (86)$$

are analyzed as a function of  $\Psi_\theta$ , with particular emphasis on its intermittent behavior. The kurtosis  $K_4(\varphi)$  is estimated via Eq. (68) by invoking the assumption of local isotropy, whereby the three components of the temperature gradient  $\nabla\vartheta \equiv (\vartheta_x, \vartheta_y, \vartheta_z)$  are treated as identically distributed.

Furthermore,  $\vartheta_x$ ,  $\vartheta_y$ , and  $\vartheta_z$  are assumed to be statistically uncorrelated. This assumption facilitates the estimation of the kurtosis of  $\varphi$  in terms of

the dimensionless statistical moments of  $\partial\vartheta/\partial r$ , yielding:

$$K_4(\varphi) = \frac{H_\theta^{(8)} - 4H_\theta^{(6)} + 6H_\theta^{(4)} - 3}{3(H_\theta^{(4)} - 1)^2} + 2 \quad (87)$$

where  $H_\theta^{(4)}$ ,  $H_\theta^{(6)}$ , and  $H_\theta^{(8)}$  are evaluated according to Eq. (68).

Figure 7 presents  $K_4(\varphi)$  as a function of  $\Psi_\theta$ , comparing the values derived from the present theory (solid line) with those obtained by [70] through nonlinear large-eddy simulations (symbols). The comparison demonstrates a qualitatively robust agreement between the datasets.

Specifically, as  $\Psi_\theta \rightarrow \infty$ , the current analysis predicts  $K_4 \rightarrow 55$ , whereas the simulations by [70] yield a value of approximately 60. This discrepancy may be attributed to the present focus on purely isotropic turbulence –which tends to constrain the dimensionless statistical moments of both  $\partial\vartheta/\partial r$  and  $\varphi$ – as well as the simplifying assumption of statistically uncorrelated temperature gradient components. Finally, it is observed that the experimental data provided by [67] and [71] allow for the identification of  $\Phi(0)$ . Table 2 reports a comparison between the value of  $\Phi(0)$  calculated via the proposed theory and those derived from the experimental results of [67] and [71]. As shown, the value of  $\Phi(0)$  computed using Eq. (71) is in excellent agreement with the values obtained from the processing of the aforementioned experimental data.

## 8. Conclusion

In this work, we have elucidated the fundamental connection between the nonlinear dynamics of the Navier–Stokes equations and the statistical

properties of velocity and temperature increments in homogeneous isotropic turbulence. The analysis demonstrates that while nonlinearity is the primary driver of intermittency, it cannot, in isolation, account for the emergence of the Kolmogorov scaling laws.

The theoretical framework is firmly rooted in the proposed closure schemes for the von Kármán–Howarth and Corrsin equations. These closures not only provide a consistent dynamical description of the energy and scalar decay but also allow for the formal identification of the transition Taylor–scale Reynolds number via specific bifurcation analysis of closed von Kármán–Howarth equation.

The central contribution of this study is the introduction of the non-observability of bifurcation modes as the essential conceptual bridge between the energy cascade and the observed statistical structure of the flow. By leveraging a decomposition into these non-observable modes and characterizing them through quasi-PDFs, we demonstrate that the synergistic effect of nonlinearity and non-observability rigorously recovers the Kolmogorov scaling laws. Specifically, we show that the ratio of the velocity standard deviation to the Kolmogorov velocity scales as  $R_\lambda^{1/2}$ . Moreover, our analysis reveals that the bifurcation modes exhibit amplitudes whose third statistical moment scales as  $R_\lambda^{-3}$ .

Significantly, the non-observability of bifurcation modes not only explains the Kolmogorov scaling law and the growing intermittency with the Taylor-scale Reynolds number, but also, and more importantly, enables the determination of the internal structure functions for velocity and temperature differences and their corresponding PDFs and statistics, which reflect very

well the existing experimental and numerical data in the literature.

By invoking Fisher principle of the minimum number of parameters (1922), we have derived a closed analytical form for the statistics of velocity and temperature increments. This framework successfully captures the growth of intermittency as a function of the Taylor–scale Reynolds number, providing a theoretical justification for the increasingly non–Gaussian behavior observed in fully developed turbulence.

The consistency between the predicted normalization coefficients, the skewness values obtained via Lyapunov analysis, and the established experimental benchmarks confirms the robustness of the proposed approach. Ultimately, these results suggest that the non–observability of bifurcation modes is not merely a mathematical convenience, but a necessary physical requirement to reconcile the intermittent nature of small–scale fluctuations with the classical universal scaling laws of turbulence.

## 9. Acknowledgments

This work was partially supported by the Italian Ministry for the Universities and Scientific and Technological Research (MIUR).

## References

- [1] RICHARDSON, L. F. (1922). *Weather Prediction by Numerical Process*. Cambridge University Press.

- [2] KOLMOGOROV, A. N. (1941). The local structure of turbulence in incompressible viscous fluid for very large Reynolds numbers. *Dokl. Akad. Nauk SSSR*, 30, 301-305.
- [3] VON KÁRMÁN, T., & HOWARTH, L. (1938). On the statistical theory of isotropic turbulence. *Proc. R. Soc. Lond. A*, 164, 192-215.
- [4] BATCHELOR, G. K., & TOWNSEND, A. A. (1949). The nature of turbulent motion at large Reynolds-numbers. *Proc. R. Soc. Lond. A*, 199, 238-255.
- [5] SREENIVASAN, K. R. (1991). On local isotropy of passive scalars in turbulent shears flows. *Annu. Rev. Fluid Mech.*, 23, 539-604.
- [6] ANSELMET, F., GAGNE, Y., HOPFINGER, E. J., & ANTONIA, R. A. (1984). High-order velocity structure functions in turbulent shear flows. *Journal of Fluid Mechanics*, 140, 63–89.
- [7] MONIN, A. S., & YAGLOM, A. M. (1975). *Statistical Fluid Mechanics: Mechanics of Turbulence*, Vol. 2. MIT Press, Cambridge, MA.
- [8] BUARIA, D., & PUMIR, A. (2020). Velocity gradient statistics in lineage of turbulent flows. *Physical Review Letters*, 124(14), 144501.
- [9] IYER, K. P., , & YEUNG, P. K. (2020). Scaling exponents of velocity structure functions in high-Reynolds-number isotropic turbulence. *Physical Review Fluids*, 5(5), 054605.
- [10] KOLMOGOROV, A. N. (1962). A refinement of previous hypotheses concerning the local structure of turbulence in a viscous incompressible

- fluid at high Reynolds number. *Journal of Fluid Mechanics*, 13(1), 77-85.
- [11] OBOUKHOV, A. M. (1962). Some specific features of atmospheric turbulence. *Journal of Fluid Mechanics*, 13(1), 77-81.
- [12] MANDELBROT, B. B. (1974). Intermittent turbulence in self-similar cascades: divergence of high moments and dimension of the carrier. *Journal of Fluid Mechanics*, 62(2), 331-358.
- [13] FRISCH, U., & PARISI, G. (1985). Fully developed turbulence and intermittency. In: *Turbulence and Predictability in Geophysical Fluid Dynamics and Climate Dynamics*, 84-88. North-Holland, Amsterdam.
- [14] FRISCH, U., SULEM, P. L., & NELKIN, M. (1978). A simple dynamical model of intermittent fully developed turbulence. *Journal of Fluid Mechanics*, 87(4), 719-736.
- [15] SHE, Z. S., & LÉVÉQUE, E. (1994). Universal scaling laws in fully developed turbulence. *Physical Review Letters*, 72(21), 3363-3366.
- [16] MENEVEAU, C. (2022). Perspectives on progress in the understanding of turbulent flows. *Physical Review Fluids*, 7(12), 120501.
- [17] JOHNSON, P. L., & MENEVEAU, C. (2023). On the Role of Dissipation and Pressure-Gradient Correlation in Velocity Gradient Evolution. *Journal of Fluid Mechanics*, 955, A20.

- [18] CORRISIN, S. (1951). On the spectrum of isotropic temperature fluctuations in an isotropic turbulence. *Journal of Applied Physics*, 22(4), 469-473.
- [19] WARHAFT, Z. (2000). Passive scalars in turbulent flows. *Annual Review of Fluid Mechanics*, 32, 203-240.
- [20] SHRAIMAN, B. I., & SIGGIA, E. D. (2000). Scalar turbulence. *Nature*, 405(6787), 639–646.
- [21] BUARIA, D., & Sreenivasan, K. R. (2022). Intermittency of passive scalars in the dissipation range of turbulent flows. *Physical Review Letters*, 128(23), 234502.
- [22] FISHER, R. A. (1922). On the mathematical foundations of theoretical statistics. *Philosophical Transactions of the Royal Society A*, 222, 309-368.
- [23] DE DIVITIIS, N., Lyapunov Analysis for Fully Developed Homogeneous Isotropic Turbulence, *Theoretical and Computational Fluid Dynamics*, (2011), DOI: 10.1007/s00162-010-0211-9.
- [24] DE DIVITIIS, N., Finite Scale Lyapunov Analysis of Temperature Fluctuations in Homogeneous Isotropic Turbulence, *Appl. Math. Modell.*, (2014), DOI: 10.1016/j.apm.2014.04.016.
- [25] DE DIVITIIS N., von Kármán–Howarth and Corrsin equations closure based on Lagrangian description of the fluid motion, *Annals of Physics*, vol. 368, May 2016, Pages 296-309, (2016), DOI: 10.1016/j.aop.2016.02.010.

- [26] DE DIVITIIS, N., Liouville spectral gap and bifurcation–driven Lagrangian–Eulerian decoupling with nondiffusive turbulence closures *Transport Phenomena* **1**, no. 1, 2026, pp. 20260015. <https://doi.org/10.1515/tp-2026-0015>.
- [27] FEIGENBAUM, M. J., *J. Stat. Phys.* **19**, (1978).
- [28] ECKMANN, J.P., Roads to turbulence in dissipative dynamical systems *Rev. Mod. Phys.* **53**, 643–654, (1981).
- [29] DE DIVITIIS N., Refinement of a Previous Hypothesis of the Lyapunov Analysis of Isotropic Turbulence, *Journal of Engineering*, vol. 2013, Article ID 653027, 4 pages, (2013), <https://doi.org/10.1155/2013/653027>.
- [30] DE DIVITIIS, N. (2019). Statistical Lyapunov Theory Based on Bifurcation Analysis of Energy Cascade in Isotropic Homogeneous Turbulence: A Physical–Mathematical Review. *Entropy*, 21(5), 520. DOI: <https://doi.org/10.3390/e21050520>
- [31] Yao, H., et al. (2025). Analysis of inertial-range intermittency in forward and inverse cascade regions in isotropic turbulence. *arXiv preprint arXiv:2504.04595*.
- [32] DE DIVITIIS, N., Self-Similarity in Fully Developed Homogeneous Isotropic Turbulence Using the Lyapunov Analysis, *Theoretical and Computational Fluid Dynamics*, (2012), DOI: 10.1007/s00162-010-0213-7.
- [33] CHEN S., DOOLEN G.D., KRAICHNAN R.H., SHE Z-S., On statistical correlations between velocity increments and locally averaged

- dissipation in homogeneous turbulence, *Phys. Fluids A*, **5**, pp. 458–463, (1992).
- [34] ORSZAG S.A., PATTERSON G.S., Numerical simulation of three-dimensional homogeneous isotropic turbulence., *Phys. Rev. Lett.*, **28**, 76–79, (1972).
- [35] PANDA R., SONNAD V., CLEMENTI E. ORSZAG S.A., YAKHOT V., Turbulence in a randomly stirred fluid, *Phys. Fluids A*, **1(6)**, 1045–1053, (1989).
- [36] ANDERSON R., MENEVEAU C., Effects of the similarity model in finite-difference LES of isotropic turbulence using a lagrangian dynamic mixed model, *Flow Turbul. Combust.*, **62**, pp. 201–225, (1999).
- [37] CARATI D., GHOSAL S., MOIN P., On the representation of backscatter in dynamic localization models, *Phys. Fluids*, **7(3)**, pp. 606–616, (1995).
- [38] KANG H.S., CHESTER S., MENEVEAU C. , Decaying turbulence in an active-gridgenerated flow and comparisons with large-eddy simulation., *J. Fluid Mech.* **480**, pp. 129–160, (2003).
- [39] BATCHELOR, G. K., Small-scale variation of convected quantities like temperature in turbulent fluid. Part 1. General discussion and the case of small conductivity, *Journal of Fluid Mechanics*, **5**, (1959), pp. 113–133
- [40] BATCHELOR G. K., HOWELLS I. D., TOWNSEND A. A., Small-scale variation of convected quantities like temperature in turbulent fluid.

- Part 2. The case of large conductivity, *Journal of Fluid Mechanics*, **5**, (1959), pp. 134–139
- [41] OBUKHOV, A. M., The structure of the temperature field in a turbulent flow. *Dokl. Akad. Nauk., CCCP*, **39**, (1949), pp. 391.
- [42] GIBSON, C. H., SCHWARZ W. H., The Universal Equilibrium Spectra of Turbulent Velocity and Scalar Fields, *Journal of Fluid Mechanics*, **16**, (1963), pp. 365–384
- [43] MYDLARSKI, L., WARHAFT, Z., Passive scalar statistics in high-Péclet-number grid turbulence, *Journal of Fluid Mechanics*, **358**, (1998), pp. 135–175
- [44] CHASNOV, J., CANUTO V. M., ROGALLO R. S., Turbulence spectrum of strongly conductive temperature field in a rapidly stirred fluid. *Phys. Fluids A*, **1**, pp. 1698-1700, (1989), doi:10.1063/1.857535.
- [45] DONZIS D. A., SREENIVASAN K. R., YEUNG P. K., The Batchelor Spectrum for Mixing of Passive Scalars in Isotropic Turbulence, *Flow, Turbulence and Combustion*, **85**, pp. 549–566, no. 3–4, (2010), DOI: 10.1007/s10494-010-9271-6
- [46] FEYNMAN, RICHARD P., *Negative Probability*, In Peat, F. David; Hiley, Basil. Quantum Implications: Essays in Honour of David Bohm. Routledge & Kegan Paul Ltd. pp. 235–248, (1987).
- [47] BURGIN M., Extended Probabilities: Mathematical Foundations, *arXiv:0912.4767*, (2009).

- [48] BURGIN M., Interpretations of Negative Probabilities, *arXiv:1008.1287*, (2010).
- [49] RUELLE, D., TAKENS, F., *Commun. Math Phys.* **20**, 167, (1971).
- [50] POMEAU, Y., MANNEVILLE, P., *Commun Math. Phys.* **74**, 189, (1980).
- [51] ARNOLD, V. I., *Catastrophe Theory*. 3rd ed. Berlin: Springer-Verlag, (1992).
- [52] ARNOLD, V.I., AFRAJMOVICH V.S., IL'YASHENKO YU.S., SHIL'NIKOV L.P., *Dynamical Systems V: Bifurcation Theory and Catastrophe Theory*. Springer Science & Business Media, (2013).
- [53] DE DIVITIIS N., Bifurcations analysis of turbulent energy cascade, *Annals of Physics*, (2015), DOI: 10.1016/j.aop.2015.01.017.
- [54] TRUESDELL, C. *A First Course in Rational Continuum Mechanics*, Academic, New York, (1977).
- [55] TSINOBER, A. *An Informal Conceptual Introduction to Turbulence: Second Edition of An Informal Introduction to Turbulence*, Springer Science & Business Media, (2009).
- [56] BATCHELOR, G.K., *The Theory of Homogeneous Turbulence*. Cambridge University Press, Cambridge, (1953).
- [57] LOÉVE, M., *Probability Theory*. Springer-Verlag, New York, (1999).

- [58] CARR, J., *Applications of Centre Manifold Theory*, Applied Mathematical Sciences. Springer-Verlag, (1981).
- [59] VENTSEL, E. S., *Theorie des probabilités*. Ed. Mir, CCCP, Moskow, (1973).
- [60] LEHMANN, E.L., *Elements of Large-sample Theory*. Springer, (1999).
- [61] DE JONG, P., A central Limit Theorem for generalized quadratic forms *Probab. Th. Rel. Fields*, **75**, 261–277 (1987).
- [62] NICOLIS, G., *Introduction to nonlinear science*, Cambridge University Press, (1995).
- [63] WISHART J. AND BARTLETT M. S., *The distribution of second order moment statistics in a normal system*, Proceedings of the Cambridge Philosophical Society, **28**, 455–459 (1932).
- [64] CASTAING B., GAGNE Y., AND HOPFINGER E. J., *Velocity probability density functions of high Reynolds number turbulence*, Physica D: Nonlinear Phenomena, **46**(2), 177–200 (1990).
- [65] CHING E. S., *Probability densities of turbulent temperature gradients*, Physical Review A, **44**(6), 3622 (1991).
- [66] KAILASNATH P., SREENIVASAN K. R. AND STOLOVITZKY G., *Probability density of velocity increments in turbulent flows*, Physical Review Letters, **68**(18), 2766 (1992).

- [67] TABELING, P., ZOCCHI, G., BELIN, F., MAURER, J., WILLAIME, H., Probability density functions, skewness, and flatness in large Reynolds number turbulence, *Phys. Rev. E* **53**, 1613, (1996).
- [68] BELIN, F., MAURER, J. WILLAIME, H., TABELING, P., Velocity Gradient Distributions in Fully Developed Turbulence: An Experimental Study, *Physics of Fluid* **9**, no. 12, 3843–3850, (1997).
- [69] SHE, Z.S., LEVEQUE, E., Universal scaling laws in fully developed turbulence *Phys. Rev. Lett.* **72**, 336, (1994).
- [70] BURTON G.C., The nonlinear large-eddy simulation method applied to and passive-scalar mixing, *Phys. Fluids*, **20**,035103, (2008), DOI: <http://dx.doi.org/10.1063/1.2840199>
- [71] SREENIVASAN K. R., TAVOULARIS S., HENRY R., CORRSIN S., Temperature fluctuations and scales in grid-generated turbulence., *Journal of Fluid Mechanics*, **100**, (1980), pp. 597–621, doi:10.1017/S0022112080001309

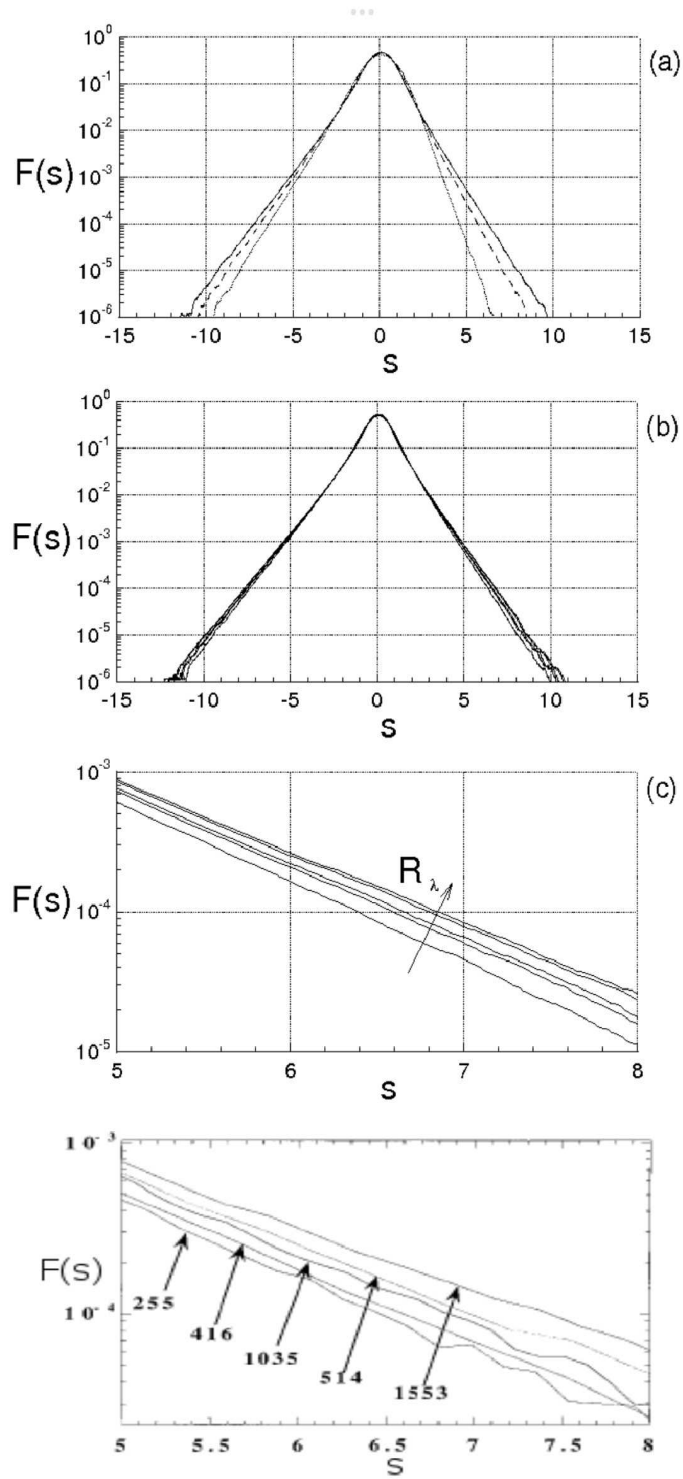


Figure 4: Top a), b), c): PDF of longitudinal velocity derivative for various values of  $R_\lambda$ . a) Dotted, dash-dotted, and continuous lines represent  $R_\lambda = 15, 30$ , and  $60$ , respectively. b) and c) PDFs for  $R_\lambda = 255, 416, 514, 1035$ , and  $1553$ . Plot (c) provides a detailed view of the tails shown in (b). Bottom: Experimental data from Ref. [67].

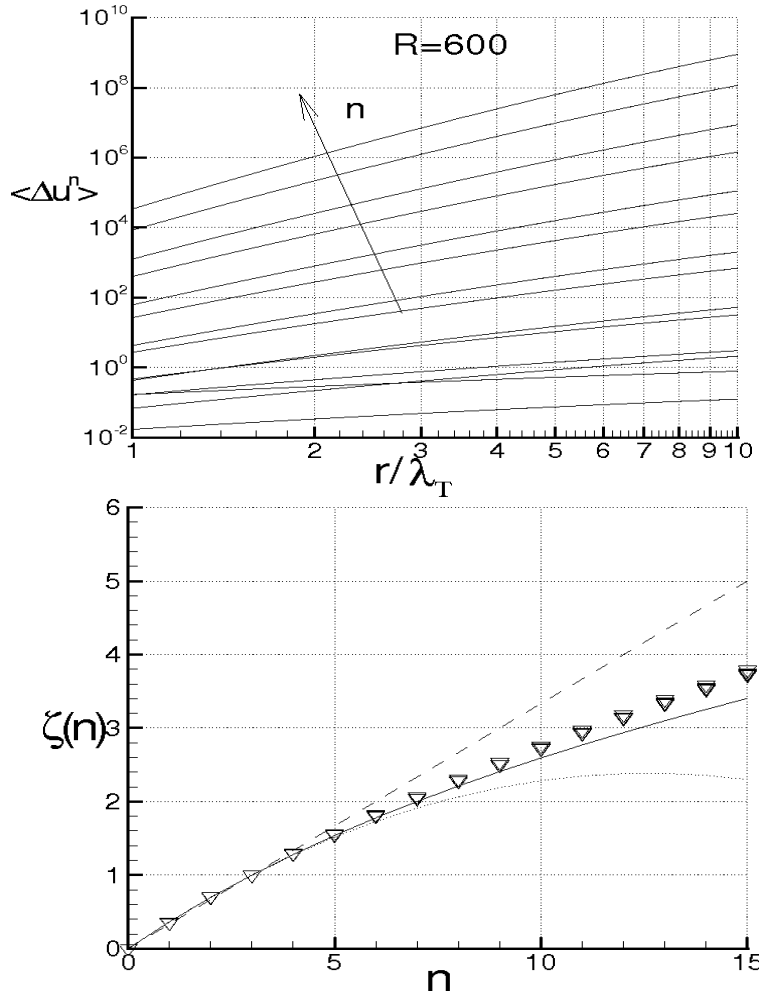


Figure 5: Top: Statistical moments of  $\Delta u_r$  as a function of the separation distance for  $R_\lambda = 600$ . Bottom: Scaling exponents of the velocity increments at different  $R_\lambda$ . Solid symbols denote data from the present analysis. The dashed line represents K41 theory [2], the dotted line denotes K62 theory [10], and the continuous line indicates the She–Leveque model [69].

Table 1: Dimensionless statistical moments of  $\partial u_r / \partial r$  at different values of the Taylor scale Reynolds numbers. P.R. as for "present results".

Moment	$R_\lambda \approx 10$	$R_\lambda = 10^2$	$R_\lambda = 10^3$	Gaussian
Order	P. R.	P. R.	P. R.	Moment
3	-.428571	-.428571	-.428571	0
4	3.96973	7.69530	8.95525	3
5	-7.21043	-11.7922	-12.7656	0
6	42.4092	173.992	228.486	15
7	-170.850	-551.972	-667.237	0
8	1035.22	7968.33	11648.2	105
9	-6329.64	-41477.9	-56151.4	0
10	45632.5	617583.	997938.	945

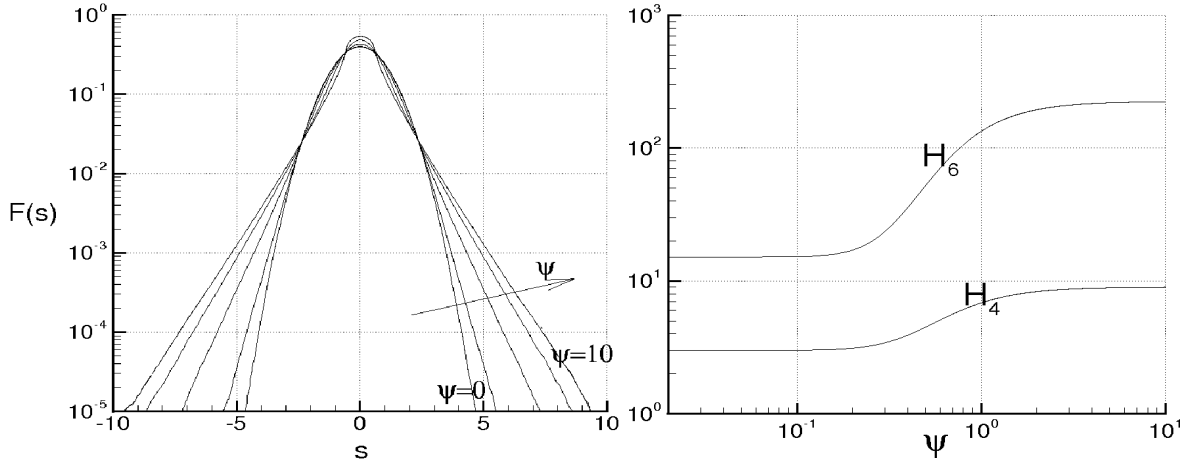


Figure 6: Left: Distribution function of the longitudinal temperature derivatives for various values of  $\Psi_\theta$ . Right: Dimensionless statistical moments  $H_\theta^{(4)}$  and  $H_\theta^{(6)}$  as functions of  $\Psi_\theta$ .

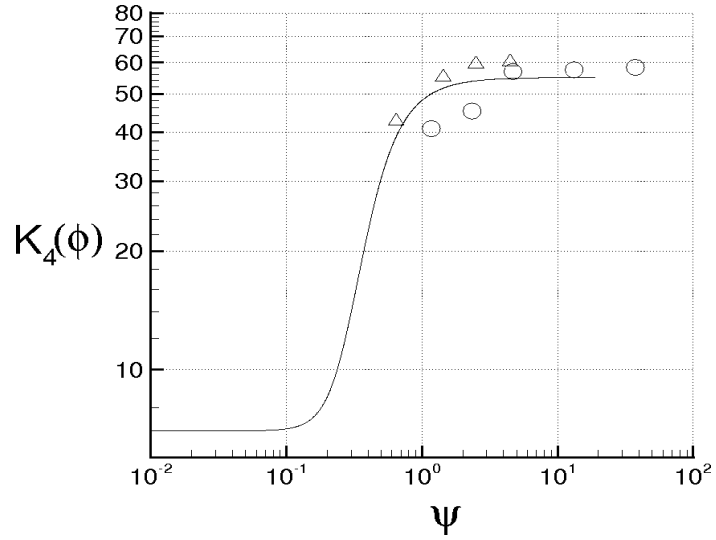


Figure 7: Comparison of the kurtosis of temperature dissipation as a function of  $\Psi_\theta$ . The symbols represent the results reported by [70].

Reference	$\Phi(0)$
Present Analysis	0.1409...
[67]	$\simeq 0.148$
[71]	$\simeq 0.135$

Table 2: Identification of  $\Phi(0)$  through the elaboration of experimental data from [67] and [71], and comparison with the present analysis.